Publicado en ACS Infect. Dis. 5, 873-891 (2019)

Pyrrolopyrimidine *vs* imidazole-phenyl-thiazole scaffolds in non-peptidic candidates to inhibit dimerization of *Leishmania infantum* trypanothione reductase

Alejandro Revuelto,[a] Marta Ruiz-Santaquiteria,[a] Héctor de Lucio,[b] Ana Gamo,[a] Alejandra A. Carriles,[c] Kilian Jesús Gutiérrez,[b] Pedro A. Sánchez-Murcia,[d] Juan A. Hermoso,[c] Federico Gago,[d] María-José Camarasa,[a] Antonio Jiménez-Ruiz,[b] and Sonsoles Velázquez[a]*

[a] *Instituto de Química Médica (IQM-CSIC), E-28006 Madrid, Spain*

[b] *Departamento de Biología de Sistemas, Universidad de Alcalá, E-28805 Alcalá de Henares, Madrid, Spain*

[c] *Department of Crystallography and Structural Biology, Institute of Physical Chemistry "Rocasolano,"(IQFR-CSIC), E-28006 Madrid, Spain*

[d] *Área de Farmacología, Departamento de Ciencias Biomédicas, Unidad Asociada al IQM-CSIC, Universidad de Alcalá, E-28805 Alcalá de Henares, Madrid, Spain*

* Corresponding author: Dr. Sonsoles Velázquez
Instituto de Química Médica (IQM-CSIC), C/ Juan de la Cierva 3
E-28006 Madrid (Spain) Phone number: (+34) 912587689
e-mail: iqmsv29@iqm.csic.es

Disruption of protein-protein interactions of essential oligomeric enzymes by small molecules represents a significant challenge. We recently reported some linear and cyclic peptides derived from an α-helical region present in the homodimeric interface of *Leishmania infantum* trypanothione reductase (*Li*-TryR) that showed potent effects on both dimerization and redox activity of this essential enzyme. Here we describe our first steps towards the design of non-peptidic small-molecule *Li*-TryR dimerization disruptors using a proteomimetic approach. The pyrrolopyrimidine and the 5-6-5 imidazole-phenyl-thiazole α-helix-mimetic scaffolds were suitably decorated with substituents that could mimic three key residues (K, Q and I) of the linear peptide prototype (PKIIQSVGIS-Nle-K-Nle). Extensive optimization of previously described synthetic methodologies was required. A library of 15 compounds bearing different hydrophobic alkyl and aromatic substituents was synthesized. The imidazole-phenyl-thiazole-based analogues outperformed the pyrrolopyrimidine-based derivatives in both inhibiting the enzyme and killing extracellular and intracellular parasites in cell culture. The most active imidazole-phenyl-thiazole compounds **3e** and **3f** inhibit *Li*-TryR and prevent growth of the parasites at low micromolar concentrations similar to those required by the peptide prototype. The intrinsic fluorescence of these compounds inside the parasites visually demonstrates their good permeability in comparison with previous peptide-based *Li*-TryR dimerization disruptors.

Keywords- α-helix mimetics, protein-protein interactions, small-molecule dimerization disruptor, trypanothione reductase, *Leishmania infantum*

Leishmaniasis is a parasitic disease caused by protozoa of the genus *Leishmania,* whose 20 recognized species can infect humans leading to three main clinical syndromes: cutaneous leishmaniasis (CL), mucocutaneous leishmaniasis (MCL) and visceral leishmaniasis (VL). VL is the most severe form of the disease, which is caused by *L. donovani* and *L. infantum* species. This disease is endemic in 98 countries where 300,000 out of more than one million of new reported cases every year belong to VL, which is responsible for around 40,000 deaths per year.[1] Unfortunately, despite being one of the major neglected tropical diseases in terms of number of cases and death rate, drug development has not kept pace with its severity and prevalence.[2-5] There is no effective vaccine for leishmaniasis[6] and currently available treatments possess several drawbacks related to high toxicity, side-effects and the emergence of resistance. All of the above caveats justify the research for novel and more effective antileishmanial drugs.

Trypanothione reductase (TryR), one of the few genetically and chemically validated drug targets in trypanosomatids (including the genus *Leishmania*), is an enzyme critical for antioxidant defense.[7-9] The trypanothione/trypanothione reductase (Try/TryR) couple is analogous to, but distinct from, its mammalian counterpart based on the glutathione/glutathione reductase (GSH/GR) pair. The absence of TryR in mammalian cells, the significant differences between the host and parasite enzymes (including opposite net charges in the active sites of the two enzymes) and its vital role for the parasite make TryR an attractive target for rational drug design.[10-12] Although a large variety of potent and selective competitive TryR inhibitors have been described that are good trypanocides *in vitro,* there are scarce reports of compounds that are also effective *in vivo*. Besides, all known inhibitors target the active site through covalent inactivation of the catalytic cysteine residues and/or electrostatic interactions with negatively charged protein residues.[13] One of the disadvantages of TryR as a target is that the survival of the parasite is only affected when its activity is reduced by more than 90%. This implies that competitive inhibitors must have a very high binding affinity. For this reason, non-competitive or irreversible inhibitors are known to be more

attractive alternatives for targeting this enzyme. Since the biologically functional form of TryR is a homodimer, our research group is pursuing an alternative inhibition strategy that attempts to disrupt protein-protein interactions (PPIs) at the homodimer interface.[14] Potential druggable sites for PPIs disruptors were explored by analysis of the interface through a combination of molecular modelling and site-directed mutagenesis. As a result, E436 was identified as a key residue for the structural integrity and catalytic activity of the enzyme. As a "proof of concept" of this novel approach we designed and tested a small library of linear peptides representing rational variations of the α-helix spanning residues P435 to M447 of *Leishmania infantum* TryR (*Li*-TryR) which contains the validated *hot spot* E436. From these studies, the 13-*mer* linear peptides PKIIQSVGICMKM (**1a**, TRL14) and the chemically stable PKIIQSVGIS-Nle-K-Nle derivative (**1b**, TRL35) emerged as potent inhibitors of both the activity and the dimerization of the enzyme at low micromolar concentrations.[14] Different peptidomimetics were later explored to stabilize the helical structure of these short peptides and increase their metabolic stability. Constrained cyclic peptides[15-17] and α/β^3-peptide foldamers[18] not only retained activity but also provided higher proteolytic stability (up to 40-fold) in comparison to their linear peptide counterparts. However, we found it necessary to prepare structurally complex conjugates with cell-penetrating peptides to facilitate cellular uptake of all the peptide-based inhibitors and, thus, kill the parasites *in vitro*.

In addition to peptide-based approaches, the development of non-peptidic α-helix mimetics that reproduce key features of short peptides for inhibiting PPIs is an active area of research.[19-22] Hamilton and coworkers first demonstrated[23] that a terphenyl scaffold substituted with appropriate functional groups can reproduce the spatial orientation of the key side-chains found predominantly at the *i*, *i+3* or *i+4* and *i+7* positions at a common face in α-helical peptides. Since this pioneering work was published, numerous terphenyl-inspired scaffolds, also termed proteomimetics, have been developed to improve water solubility, synthetic accessibility, and/or flexibility.[20,24,25] To increase the water solubility, the strategy of benzene-to-heterocycle replacement leading to more hydrophilic

and/or amphiphilic scaffolds (e.g. terpyridine, terephthalamide or 5-6-5 imidazole-phenyl-thiazole scaffolds)[26-29] has been widely used. The synthetic difficulty can be reduced by using solid-phase methods (e.g. *N*-alkylated oligobenzamide or pyrrolopyrimidine scaffolds)[30-33] or multicomponent reactions (e.g. phenyl-imidazole-phenyl).[34] The conformational flexibility can be restricted by intra-molecular hydrogen bonds (e.g. terephthalamide, trispyridylamide or enaminone scaffolds). Interestingly, several proteomimetics were shown to disrupt α-helix-mediated PPIs *in vitro* and *in vivo* thus highlighting a great therapeutic potential.[25,35,36]

Here we describe our first steps in the rational design of small-molecule non-peptidic TryR dimerization inhibitors with enhanced drug-like properties that mimic the key interactions between the prototype peptide and the enzyme and hence produce the same biological effects. Alanine-scanning studies and molecular dynamics (MD) simulations of a *Li*-TryR monomer in complex with the peptide prototype **1b** (TRL35) suggested that the side-chains of residues Lys-2, Gln-5 and Ile-9 located at *i*, *i+3* and *i+7* positions, respectively, of the helical peptide may have large contributions to the inhibitory potency.[14] Since these residues are arranged on the same face of the α-helix we thought that they should be suitable for a proteomimetic replacement approach (Figure 1a,b). From the diverse array of scaffolds reported in the literature to mimic an α-helix, we focused on pyrrolopyrimidines[32] and 5-6-5 imidazole-phenyl-thiazoles[28,29] because of their synthetic accessibility, conformational rigidity and water solubility. Target proteomimetics **2a-i** and **3a-e** bearing a variety of Lys, Gln and Ile side-chains mimetic substituents were synthesized (Figure 1c). The biological evaluation of these two novel families of small-molecule TryR inhibitors in activity/dimerization enzymatic assays and their *in vitro* leishmanicidal effects against promastigotes and extracellular and intracellular amastigotes of *Leishmania infantum* was also undertaken. The water solubility of the most potent inhibitors was also experimentally measured. In addition, the structure of the complex between *Li*-TryR and pyrrolopyrimidine **2f** solved by X-ray crystallography revealed a binding site for this novel TryR inhibitor.

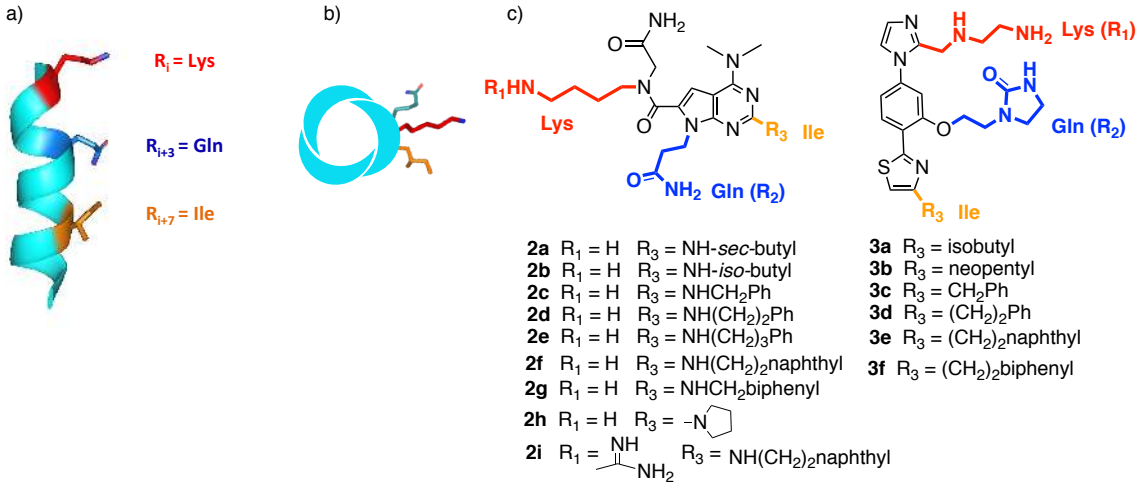

Figure 1. a) Selected lysine (**Lys**), glutamine (**Gln**) and isoleucine (**Ile**) residues corresponding to positions *i*, *i+3* and *i+7* in the prototype peptide **1b**; **b)** These residues are located on the same face of the helix; c) Target proteomimetics **2a-i** and **3a-f** based on a pyrrolopyrimidine or a 5-6-5 imidazole-phenyl-thiazole scaffold, respectively.

RESULTS AND DISCUSSION

Chemistry. The proposed proteomimetic structures **2** and **3** incorporate, in addition to the hydrophobic side chain of Ile, mimics of the charged and polar side-chains of residues Lys and Gln. This area of α-helix mimicry for PPI modulation has not been as extensively explored as that involving hydrophobic or aromatic replacements. The present study represents an example of the synthetic difficulties encountered in the application of previously described methodologies to our particular side-chains. Thus, for the preparation of the target compounds, alternative routes and/or extensive optimization of reaction conditions were required.

Synthesis of pyrrolopyrimidine derivatives ***2a-i*** (Figure 1). The pyrrolopyrimidine scaffold designed by H-S. Lim *et al.*[32,33] is attractive due to its synthetic accessibility *via* a solid-phase synthesis, its increased conformational rigidity and its favorable physical properties such as water solubility and cell permeability. The synthesis of target pyrrolopyrimidine **2a** bearing the R_1, R_2, and R_3 substituents that mimic the Lys, Gln and Ile residues, respectively, was first attempted following the described solid-phase methodology.[32] Thus, introduction of the first two functionalities (R_1 and R_2 substituents) (Scheme 1) was followed by on-resin cyclization to generate

the pyrrolopyrimidine ring, and finally the nucleophilic substitution of a sulfone group with amines to introduce the R_3 substituent (Scheme 1). The reactions were monitored by HPLC-MS after cleavage of small quantities of the resin. Thus, bromo acetylation of the amine group on Rink amide resin (Scheme 1) followed by displacement of the bromide with *N*-Boc-1,4-butanediamine (Lys mimetic R_1 substituent) yielded the peptoidyl-resin intermediate **5**. Repeating the same procedure with the 3-aminopropanamide Gln mimetic (R_2 substituent) provided the Boc-protected dimeric peptoid resin **6** quantitatively. Nucleophilic substitution of **6** with commercially available 4,6-dichloro-2-methylthio-5-formylaldehyde (**7**) afforded aldehyde intermediate **8**. Dimethylamination followed by base-induced cyclization of the resin-bound aldehyde, in the presence of DBU in DMF and MeOH at 90 °C, furnished the pyrrolopyrimidine peptidyl-resin **9** with no traces of starting material or iminium intermediates. Next, oxidation of the thioether group of **9** with *meta*-chloroperbenzoic acid, in the presence of $NaHCO_3$, provided sulfone intermediate **10** in excellent conversions by HPLC-MS (Scheme 1). However, unexpectedly, all attempts of nucleophilic substitution of the sulfone intermediate **10** with *sec*-butylamine (Ile mimetic R_3 substituent) in the presence of DIEA in NMP at 170 °C to give the final compound **2a** failed. Different temperatures (150-190 °C) and bases (DIEA, TEA, DBU) were used but only complex mixtures of decomposition products or unreacted starting material were detected by HPLC-MS after final standard TFA cleavage of the resin. It seems that the high-temperature conditions required for the nucleophilic substitution reaction with amines in resin **10** is not compatible with the presence of our selected charged/polar substituents R_1 and R_2.

Scheme 1. Initial attempts of synthesis of pyrrolopyrimidine 2a following reported method[a]

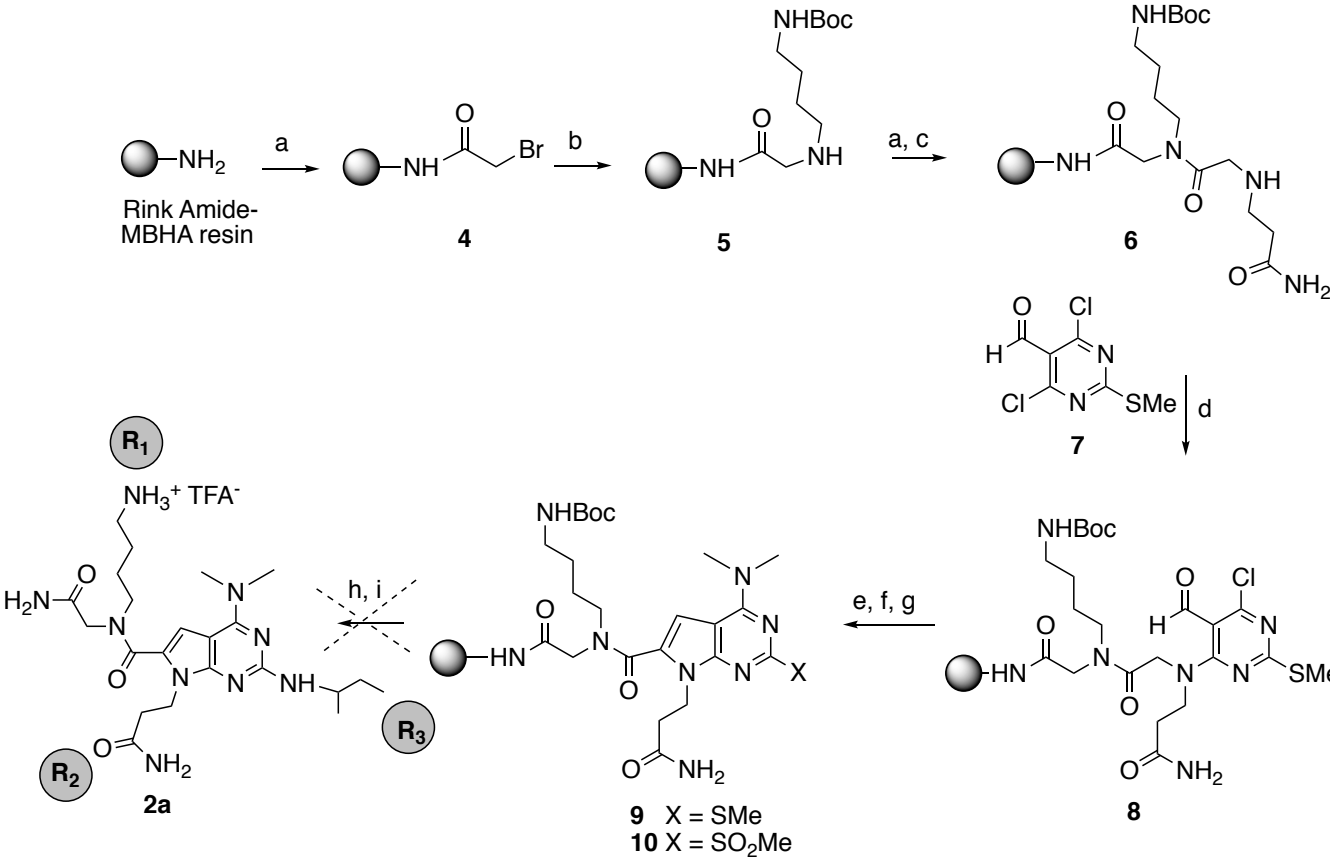

[a]Reagents and conditions: (a) $BrCH_2CO_2H$, DIC, DMF, rt; (b) $H_2N(CH_2)_4NHBoc$,DMF, rt; (c) H_2N-$(CH_2)_2CONH_2$, DIEA, DMSO, rt; (d) **7**, TEA, THF, rt; (e) NMe_2, NMP, 60 °C; (f) DBU, DMF, MeOH, 90 °C; (g) mCPBA, $NaHCO_3$, DCM, rt; (h) *sec*-$BuNH_2$, DIEA/NMP, 170 °C; (i) TFA, TIPS, H_2O, rt

Next, we devised an alternative strategy (Scheme 2) using a combination of solution and modified solid-phase methodologies originally described by H-S. Lim *et al*.[32,33] This involves the initial introduction of the R_3 hydrophobic substituent in solution, through the nucleophilic substitution of commercially available 2,4,6-trichloropyrimidine-5-carbaldehyde **11** with the appropriate primary amines, followed by a second nucleophilic substitution reaction with the previously obtained resin-bound peptoid **6**, amination and final cyclization (Scheme 2). Thus, treatment of **11** with *sec*-butyl amine in the presence of DIEA at -78 °C for 3 h gave a mixture of the regioisomers substituted at 2- or 4-position **12a** (minor) and **13a** (major) which were easily separated by chromatography (Scheme 2). All the attempts to increase the **12a**/**13a** ratio by using higher temperatures, longer reaction times or other bases failed since side-products such as disubstituted derivatives or decomposition products were detected. Then, the resin-bound dimeric peptoid **6** was reacted with

4,6-dichloro-2-*sec*-butylamine-pyrimidine-5-carbaldehyde **12a** to afford aldehyde intermediate **14a**. Amination of **14a** with dimethylamine in NMP at 60 °C, subsequent cyclization with DBU at 90 °C and final acidolytic TFA cleavage from the resin furnished the desired proteomimetic **2a** in 22% overall yield after purification on a Biotage using a reverse-phase column. Similarly, target pyrrolopyrimidines **2b-h,** bearing a variety of aliphatic and aromatic groups at R_3 substituent, were obtained from the corresponding 2-substituted-4,6-dichloropyrimidine carbaldehydes **12b-h** and Boc-protected peptoidyl resin **6** in 10-57% overall yields after chromatographic purification. Finally, the guanidine analogue **2i** was prepared following a similar procedure from the Alloc-protected peptoidyl-resin **6'** and 4,6-dichloro-2-naphthylethylamine-pyrimidine-5-carbaldehyde **12f** followed by dimethylamination and cyclization to give the Alloc-protected resin **16'f**. Next, the allyl group was removed with $Pd(PPh_3)_4$ and $PhSiH_3$ as an allyl scavenger and the free primary amine group was transformed into guanidine by treatment with di-Boc-triflylguanidine in the presence of TEA. Final cleavage from the resin furnished the target guanidine pyrrolopyrimidine **2i** in low overall yield after flash purification on the Biotage.

Scheme 2. Synthesis of intermediates 12a-g (in solution) and pyrrolopyrimidines 2a-i (solid-phase)[a]

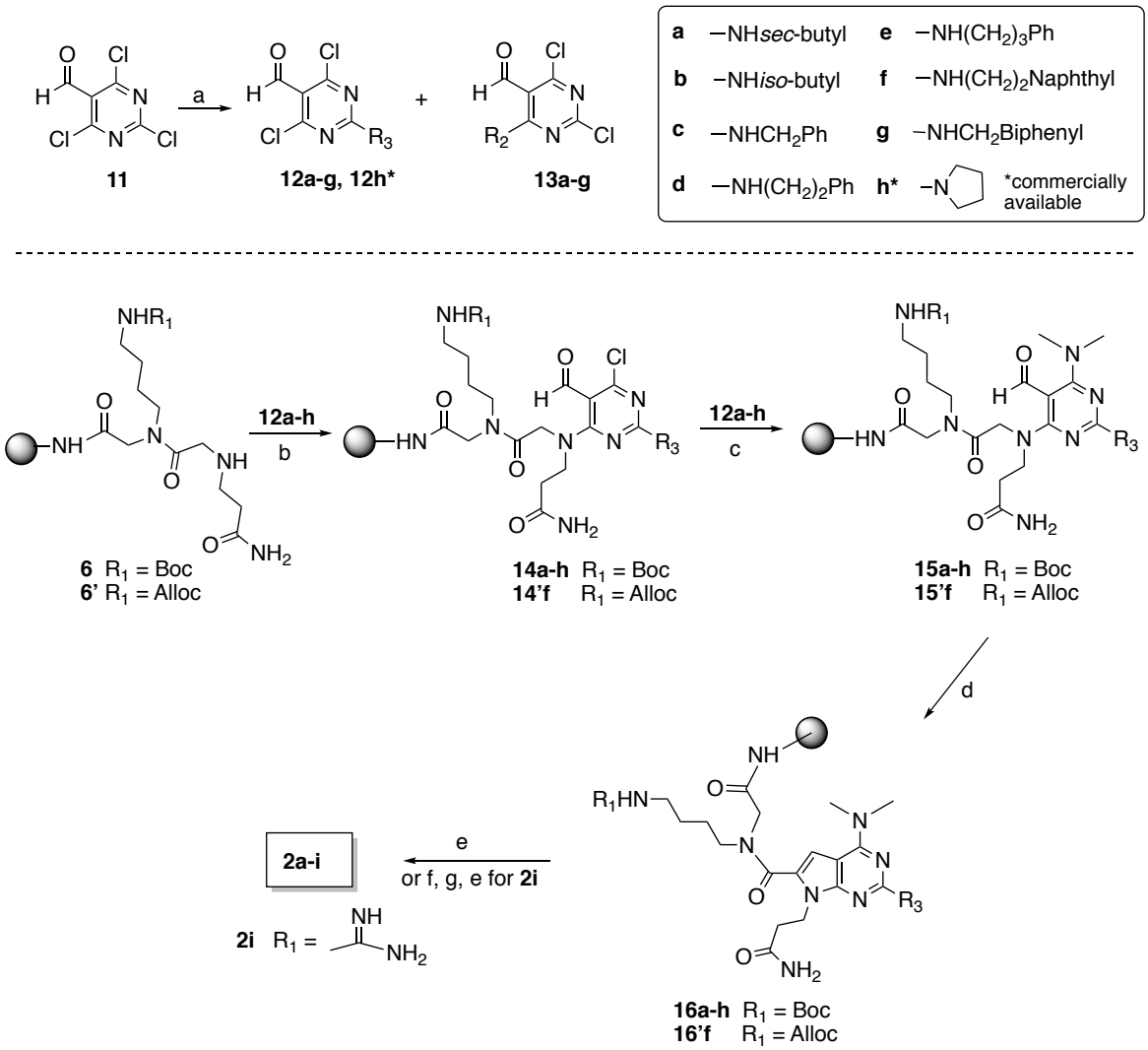

[a]Reagents and conditions: (a) R_2NH_2, DIEA, dry DCM, -78 °C; (b) **12a-h**, TEA, THF, rt; (c) NMe_2, NMP, 60 °C; (d) DBU,DMF, MeOH, 90 °C; (e) TFA, TIPS, H_2O, rt; (f) $Pd(PPh_3)_4$, $PhSiH_3$, DCM, rt; (g) 1,3-Di-Boc-2-(trifluoromethylsulfonyl)guanidine, TEA, DCM, rt

Synthesis of 5-6-5 imidazole-phenyl-thiazole derivatives ***3a-f*** (Figure 1). The 5-6-5 imidazole-phenyl-thiazole scaffold described by Hamilton and co-workers[28] replaces the phenyl end units of the original terphenyl scaffold with water-soluble five-membered heterocyclic groups. The reported synthetic route, in solution, is flexible and allows the introduction of a variety of R_1-R_3 substituents (including mimics of charged and polar side-chains) *via* high-yielding nucleophilic aromatic substitution (SN_{Ar}) of aryl fluorides with alcohols, Ullman coupling and Hantsch thiazole syntheses.[28] Initial attempts of SN_{Ar} of commercially available 4-bromo-2-fluorobenzonitrile (**17**) with 3-hydroxypropanamide (R_2 substituent to mimic the Gln residue) using KHMDS as the base,

failed to provide the desired compound **18** but instead gave phenol **19** (Scheme 3). The formation of this compound could be explained by abstraction of the acidic alpha hydrogen adjacent to the carboxamide group in the presence of a strong base (KHDMS) followed by intramolecular elimination of the phenol **19** and acrylamide. Similar side-reactions have been reported with aryl ethers in the presence of a strong base.[37]

Scheme 3. SN_{Ar} with aryl fluoride 17 or 21 and alcohols to introduce the Gln mimetic side-chain[a]

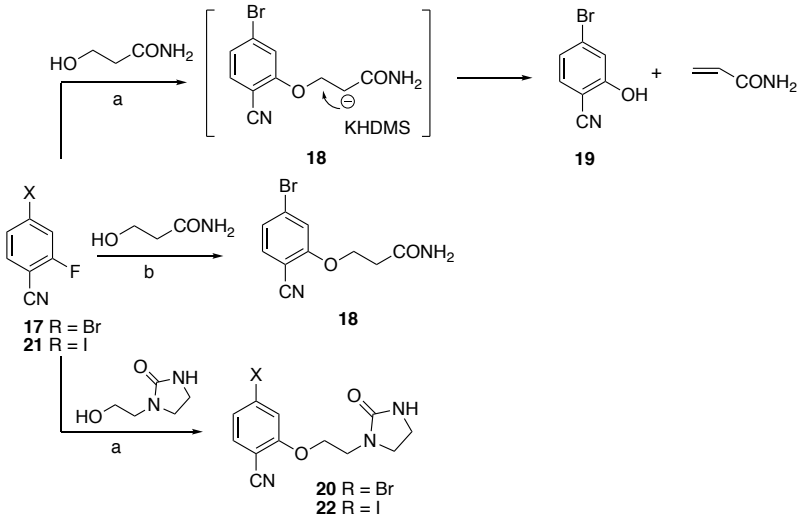

[a]Reagents and conditions: (a) KHDMS, dry THF, rt; (b) Cs_2CO_3, dry DMF, rt

Although this elimination reaction was partly reduced by the use of a weaker base such as Cs_2CO_3 to give the desired compound **18** in 30% yield, the base-sensitive nature of the compound and the unsatisfactory yield for an initial step of the synthetic pathway prompted us to explore other Gln mimetics (R_2) with no acidic protons to avoid this side reaction. Thus, reaction of **17** with 1-(2-hydroxyethyl)imidazolin-2-one in the presence of KHDMS in dry THF provided the desired compound **20** in much higher yields (71%) (Scheme 3). Similarly, the iodide derivative **22** was obtained in 83% yield from commercially available 4-iodo-2-fluorobenzonitrile (**21**) and the cyclic alcohol derivative.

Our next step involved incorporation of a Lys mimetic (R_1 substituent) onto an imidazole ring and subsequent Ullman coupling with bromide **20** (Scheme 4). Imidazole **24** was easily synthesized

by reductive amination of commercially available imidazole-5-carboxaldehyde (**23**) with N-Boc-ethylenediamine using $NaBH_4$ in 79% yield.

Scheme 4. Synthesis of imidazole-phenyl-thiazoles 3a-f and α-bromoketones 32-35[a]

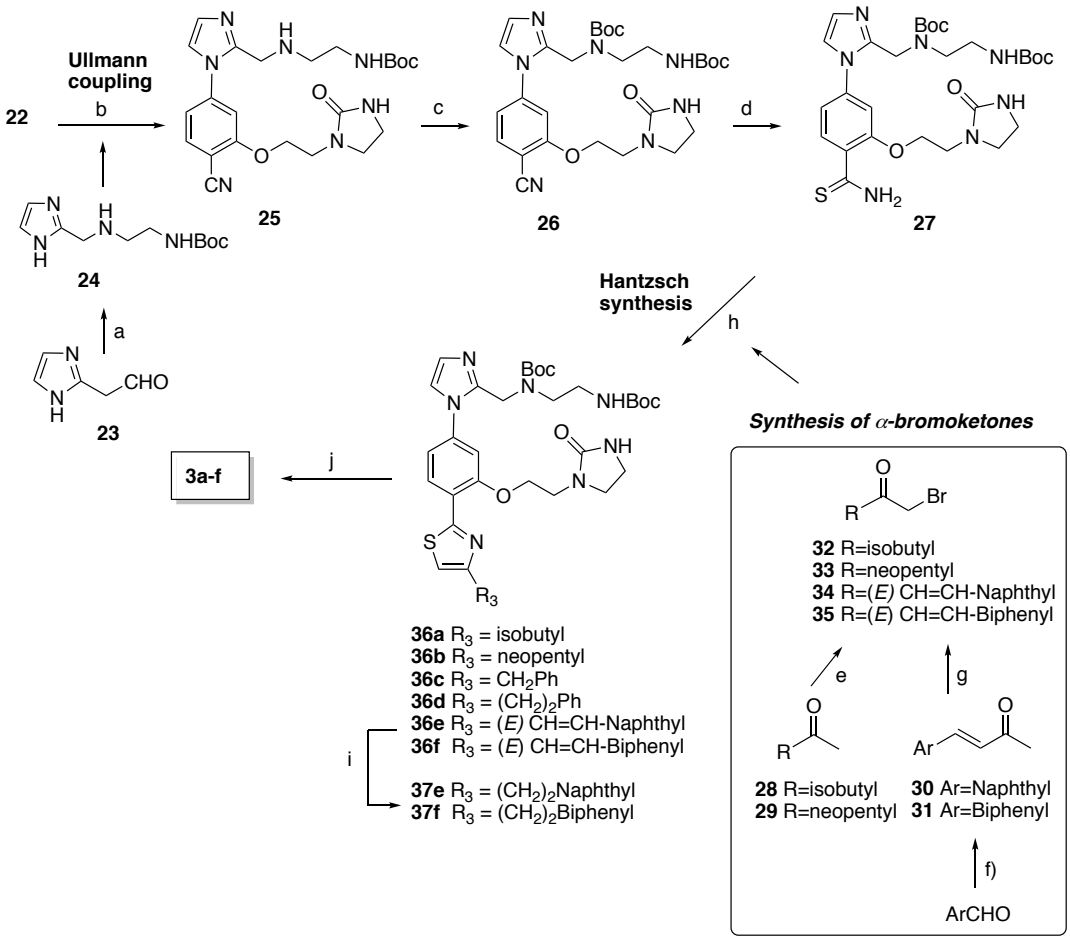

[a]Reagents and conditions: (a) i) $H_2N(CH_2)_2NHBoc$, MeOH, rt; ii) $NaBH_4$, rt; (b) imidazole **24**, *N*,*N*-dimethylglycine, Cs_2CO_3, Cu_2O, DMSO, 85 °C, MW; (c) $(Boc)_2O$, TEA, MeOH, rt; (d) $(NH_4)_2S$, DMF, 80 °C; (e) **28** and **29**, Br_2, MeOH, 0 °C; (f) ArCHO, acetone, NaOH 10%, MeOH, rt; (g) **30** or **31**, NBS, *p*-TsOH, acetonitrile, rt; (h) commercially available $BrCH_2CO(CH_2)_nPh$ (n=1,2) or synthetic α-bromoketones **32-35**, ^iPrOH, 70 °C; (i) H_2 (ballon), Pd/C 20%, THF/MeOH 1:1, rt; (j) TFA, DCM, rt

Attempts were made to couple bromide **20** with imidazole **24** via the C-N Ullman-type conditions described by Hamilton *et al*,[28] but no coupling product was observed. Different reaction conditions modifying a variety of reaction parameters[38] such as the copper source (CuI and Cu_2O), different N-O, N-N and O-O bidentate ligands (e.g. L-proline, *N*,*N*-dimethylglycine, 4,7-dimethoxy-1,10-phenantroline and dipivaloylmethane), different bases (K_2CO_3 and Cs_2CO_3), temperatures or microwave assistance were all unsuccessful. However, the desired coupling product **25** was succesfully obtained from the more reactive aryl iodide derivative **22** (Scheme 4). Thus,

treatment of **22** with imidazole **24** in the presence of Cu_2O, *N*,*N*-dimethylglycine[39] in DMSO at 85 °C, under microwave irradiation for 2 h, furnished the desired coupling product **25** in 87% yield after chromatographic purification. To avoid side reactions in the following steps of the synthesis, protection of the secondary amine with *tert*-butoxycarbonyl group (Boc), using Boc_2O in TEA at room temperature, afforded the di-Boc protected derivative **26** in excellent yield after purification. Subsequent treatment with aqueous 20% ammonium sulfide at 80 ºC for 4 h furnished the thioamide **27** in quantitative yield. Finally, Hantsch thiazole synthesis from appropriate α-bromomethylketones and the thioamide **27** facilitated late-stage attachment of a variety of alkyl and aryl R_3 substituents onto the 1,3-thiazole ring to mimic the hydrophobic side-chain of Ile residue. The synthesis of non-commercially available α-bromoketone intermediates **32-35** was performed by bromination of the corresponding methylketones using two different methodologies. For aliphatic methylketones **28** and **29**, bearing one of the alpha carbonyl positions hindered by a bulky group, reaction with Br_2 at 0 °C allows the regioselective halogenation of the end-terminal position providing compounds **32** and **33** in 68% and 52% yield, respectively. When both α-carbonyl positions were not differentiated for halogenation (i.e. aromatic ethyl methyl ketones), the strategy consisted of the use of the corresponding α/β-unsatured precursors **30** and **31,** previously synthesized by Claisen-Schmidt condensation of arylaldehydes and acetone, in the presence of NaOH in good yields. Subsequent regioselective bromination of the α-methyl group of **30** and **31** with *N*-bromosuccinimide in *p*-TsOH[40] afforded the desired α/β-unsaturated aryl α-bromomethyl ketones **34** and **35** in 46% and 42% yields, respectively after chromatographic purification. Next, Hantzsch thiazole synthesis of thioamide **27** with commercially available or previously synthesized α-bromoketones **32-35**, heating for 4 h, gave "decorated" thiazoles **36a-f** in good to excellent yields (69-95%). In the case of α/β-unsatured derivatives **36e,f** an additional step was necessary to reduce the double bond (H_2, Pd/C) so as to obtain the saturated arylethyl analogues **37e,f** in 70% and 80%

yields. Finally, treatment of di-Boc-protected intermediates (**36a-d** and **37e,f**) with TFA in DCM for 2-3 h at room temperature furnished the target proteomimetics **3a-f** quantitatively.

Proteomimetics based on the imidazole-phenyl-thiazole scaffold **3a-f** exhibited more potent TryR inhibition and leishmanicidal activity than did the pyrrolopyrimidine analogues **2a-i** (see below). We next measured the aqueous termodynamic solubilities of the most active compounds **3a-f** at 25 °C after 24 h (Supplemental Table S1). All the compounds within this series, in consonance with the predicted negative values of cLogP (range from -0.7 to -3.2), showed excellent water solubility (≥ 25 mg/mL) including **3e** and **3f**, which bear bulky aromatic R_3 substituents (naphthyl or biphenyl) on the thiazole moiety. According to the United States Pharmacopeia solubility criteria (USP 30/NF 25), the compounds can be classified as very soluble since <1 parts of solvent are required for one part of solute. Interestingly, the biologically more active imidazole-phenyl-thiazole derivatives **3a-f** displayed intrinsic fluorescence that could be used for imaging and localization of the compounds inside the parasites. Compound **3d** exhibited an absorption spectrum with a maximum at 320 nm and a single emission band at 364 nm in the blue region of the visible spectrum (Supplemental Figure S1).

Biological and structural results.

Enzymatic assays. The effect of all the compounds on the oxidoreductase activity[41] and dimeric status[14] of *Li*-TryR was evaluated using prototype peptide **1** and mepacrine as positive controls. According to the results shown in Table 1, compounds **2a-i** (based on a pyrrolopyrimidine scaffold) are significantly less potent than their imidazole-phenyl-thiazole counterparts. In the pyrrolopyrimidine series, modifications at the hydrophobic R_3 substituent (Ile mimetic) are relevant for TryR inhibitory activity. Thus, the presence of an alkyl or a benzylamino substituent at R_3 or a pyrrolidinyl (**2a-c** and **2h**) leads to inactive compounds. Interestingly, replacement of the benzyl group at R_3 by a phenylethyl or a phenylpropyl group (**2d** and **2e**), and especially the use of large

polycyclic aromatic rings (i. e. naphthyl **2f** or biphenyl **2g**), resulted in the best compounds of this series with moderate micromolar IC_{50} values. Replacement of the positively charged amino group at the R_1 substituent (Lys mimetic) by a guanidinium group in naphthyl derivatives (**2f** *vs* **2i**) slightly increased the TryR inhibitory activity.

In the imidazole-phenyl-thiazole series, all the compounds (**3a-f**) showed *Li*-TryR inhibitory activity irrespectively of the alkyl or aromatic nature of the R_3 substituent. As observed in the pyrrolopyrimidine series, introduction of a bulky hydrophobic aromatic group at R_3 clearly enhances *Li*-TryR inhibition. The naphthyl and biphenyl analogues **3e** and **3f**, with IC_{50} values in the low micromolar range, were the most potent *Li*-TryR inhibitors of the entire series.

However, the activity of the proteomimetic compounds as disruptors of *Li*-TryR dimerization is much lower than that observed for the prototype peptide **1** (Table 1). Interestingly, only the most potent inhibitors of redox activity, *i.e.* **2i**, **3e** and **3f**, showed a moderate effect on the enzyme dimerization status at 20 μM (14%, 26% and 32% reduction, respectively).

Table 1: IC_{50} ± SEM values for compounds **2a-i** and **3a-f** in the *Li*-TryR oxidoreductase activity and dimerization assays.

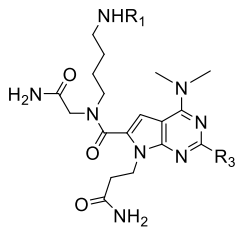

2a-i

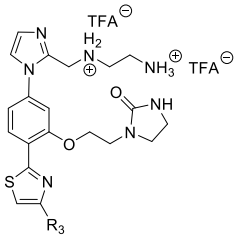

3a-f

Comp	**R_1** (TFA)	**R_3**	**IC_{50} activity (μM)[a]**	**Dimerization inhibition at 20 μM [b]**
peptide **1**	/	/	1.2 ± 0.2	95 %
Mepacrine	/	/	12.9 ± 0.5	0 %

2a	H	NH-*sec*-butyl	No inhibition	0 %
2b	H	NH-isobutyl	No inhibition	0 %
2c	H	NH-CH_2Ph	No inhibition	0 %
2d	H	NH-$(CH_2)_2$Ph	100.2 ± 13.5	0 %
2e	H	-NH-$(CH_2)_3$Ph	94.6 ± 6.4	0 %
2f	H	NH-$(CH_2)_2$Naphthyl	52.2 ± 1.8	0 %
2g	H	NH-CH_2Biphenyl	51.7 ± 5.7	0 %
2h	H	Pyrrolidinyl	No inhibition	0 %
2i	(C=NH)N H_2	NH$(CH_2)_2$-Naphthyl	39.9 ± 6.8	14 %
3a	H	isobutyl	51.2 ± 4.6	0 %
3b	H	neopentyl	51.3 ± 6.1	0 %
3c	H	CH_2-Ph	32.8 ± 2.3	0 %
3d	H	$(CH_2)_2$-Ph	22.4 ± 2.2	0 %
3e	H	$(CH_2)_2$-Naphthyl	5.1 ± 0.4	26 %
3f	H	$(CH_2)_2$-Biphenyl	8.6 ± 1.4	32 %

[a] Enzymatic activity according to a modified assay described by Hamilton et al.[41] Results are representative of three independent experiments each performed in triplicate. [b] Dimer quantitation assay (ELISA).[14]

Crystal structure of Li-TryR in complex with 2f. Attempts to co-crystallize the most potent TryR inhibitors **3e** and **3f** with the enzyme failed due to quasi-complete protein precipitation.

Incubation of *Li*-TryR with **3e** and **3f** (concentration of the inhibitors ranging from equimolar to 10-fold the molarity of TryR, for periods of 2 to 16 h, 4 ºC) resulted in strong protein precipitation and no formation of crystals, in agreement with the moderate effect of both inhibitors as dimerization disruptors.

To study the potential binding site of **2a-i** compounds in *Li*-TryR, soaking experiments were performed with *Li*-TryR crystals using the **2f** ligand, which does not disrupt the TryR dimer (Table 1). The crystal structure of the *Li*-TryR:**2f** complex, solved at 3.3 Å resolution (Supplemental Table S2 and Figure 2), displayed a nice electron density for **2f** (Supplemental Figure S2). The final model contains a TryR functional dimer consisting of two subunits related by a non-crystallographic two-fold axis. Interestingly, only chain B presents one **2f** molecule bound to its active site. The **2f** ligand is placed close to the catalytic Cys residues (Cys52 and Cys57) and to the FAD cofactor (Figure 2B). The central pyrrolopyrimidine core makes a stacking interaction with Trp21 (Figure 2B) at the so-called polyamine-binding site, where its natural substrate Try usually binds, and where a mepacrine inhibitor has also been previously localized.[42] Substituens R_1 and R_2 also play an important role in the stabilization of **2f** at *Li*-TryR by establishing different polar interactions with the protein. Thus, the Glu18 side chain and backbone atoms of Leu17 residues establish H-bond interactions with the amide moiety and keto groups in R_1, respectively. Another residue involved is Ser109, which interacts with the amide group of the glutamine mimetic in R_2. Moreover, the lysine mimetic substituent forms ion-dipole interactions with water molecules positioned in the active site of *Li*-TryR. The naphthalene ring in R_3 protrudes out of the cavity and its electron density is poorly defined, indicating high mobility in this region.

The ligand-protein interaction does not seem to dramatically alter the structure of the monomer as both independent monomers, chains B and A (with and without ligand respectively), are very similar (rmsd of 0.42Å). Changes observed between the backbone of both chains (Supplemental Figure S3A) are concentrated in different loops and at the N-terminal tail. **2f** interaction at the

active site only provokes a re-orientation of side chains of those residues directly involved in its stabilization (Supplemental Figure S3B).

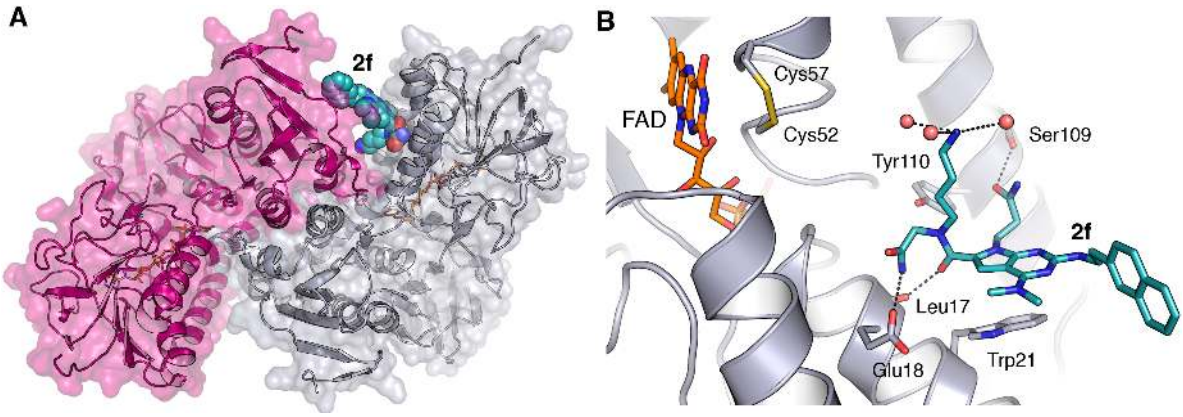

Figure 2. Three-dimensional structure of the *Li*-TryR:**2f** complex. (**A**) Molecular surface of the *Li*-TryR dimer in complex with **2f** (cyan spheres). The enzyme's backbone is depicted as a cartoon and its cofactor FAD in orange sticks. Each monomer is colored differently (grey for chain B and magenta for chain A). (**B**) Close-up view of the binding site of **2f**. The ligand prevents trypanothione from fitting into the cavity. Polar interactions are represented by dashed lines. Relevant amino acids are depicted as capped sticks and labeled. Water molecules represented as red spheres.

When the crystal structure of *Li*-TryR in complex with **2f** is best-fit superimposed onto published structures of TryR from *Trypanosoma brucei* (*Tb*-TryR), either covalently bonded to a quinacrine mustard (Supplemental Figure S4A) or in complex with cyclohexylpyrrolidine inhibitors RD0 and RD7[43] bound to the so-called 'mepacrine site' (Figure S4B), the only common interaction observed to all inhibitors involves the side chain of Trp21 in *Li*-TryR. The fact that all of them occupy the active site strongly suggests that they all prevent the binding/exit of Try.

Computational studies. Pharmacophore for pyrrolopyrimidine compounds 2. The fact that in our *Li*-TryR:**2f** co-crystal structure the naphthalene moiety is projected towards the solvent makes it difficult to extract SAR features for activity in the pyrrolopyrimidine series **2**. Moreover, it is known that the large active site of this enzyme allows a multitude of different orientations for small-molecule ligands. This fact hampers the rationalization of the activity data on the basis of a single

crystal structure for one complex.[44] For this reason, a pharmacophore model for compounds **2a**-**2i** (considering only **2f**, **2g** and **2i** as active) was constructed based on four features: aromatic (AR), hydrophobic (H), hydrogen-bond acceptor (HBA) and hydrogen-bond donor (HBD). The model showed (Figure S5) that the presence of a bulky aromatic group in the H+AR region this position is critical for *Li*-TryR dimer disruption and enzyme inhibition.

MD simulations for imidazole-phenyl-thiazole 3f bound at the dimer interface. We run classical MD simulations in explicit solvent for a *Li*-TryR monomer with **3f**, the most potent compound of series **3**, bound at the dimerization interface (Figure 3A). As the reference system, we simulated the 13-*mer* **1a** (TRL14), with capping groups at both *N*- and *C*-termini and a Lys residue at position 2 (Figure 3B).[14,16] Both systems were stabilized after a few ns of MD simulation and the root-mean squared deviation (RMSd) evolved softly along the 100-ns trajectory (Figure 3C). The interactions of the imidazolone of **3f** with the loop where Ile458 and Val460 are located were quite stable along the MD simulation and of the same order as those found for the Q5-containing peptide TRL14 (**1a**). The van der Waals contributions stand out as the main component of the drug:monomer binding energies in both cases (Figure S6). Hydrophobic residues Val460 and Ile437 are the two residues that contribute the most to the total binding energy of **3f**, closely followed by Phe454, Thr457 and Leu468 (Figure S6). The biphenyl group of this molecule occupies a large hydrophobic pocket lined by the residues shown as spheres in Figure 3A. The size of this hydrophobic site can account for the fact that derivatives **3a**-**d**, which lack large and bulky aromatic groups, do not behave as enzyme dimerization disruptors. Finally, the direct hydrogen bonds between the side-chain carboxylate of Asp432 and either the ammonium group on the imidazole side chain of **3f** or the K2 of **1a** are not constant along the trajectory (Figure 3C). This is because the ligands' positively charged groups establish alternative salt bridging interactions with Glu466 and Glu436, respectively.

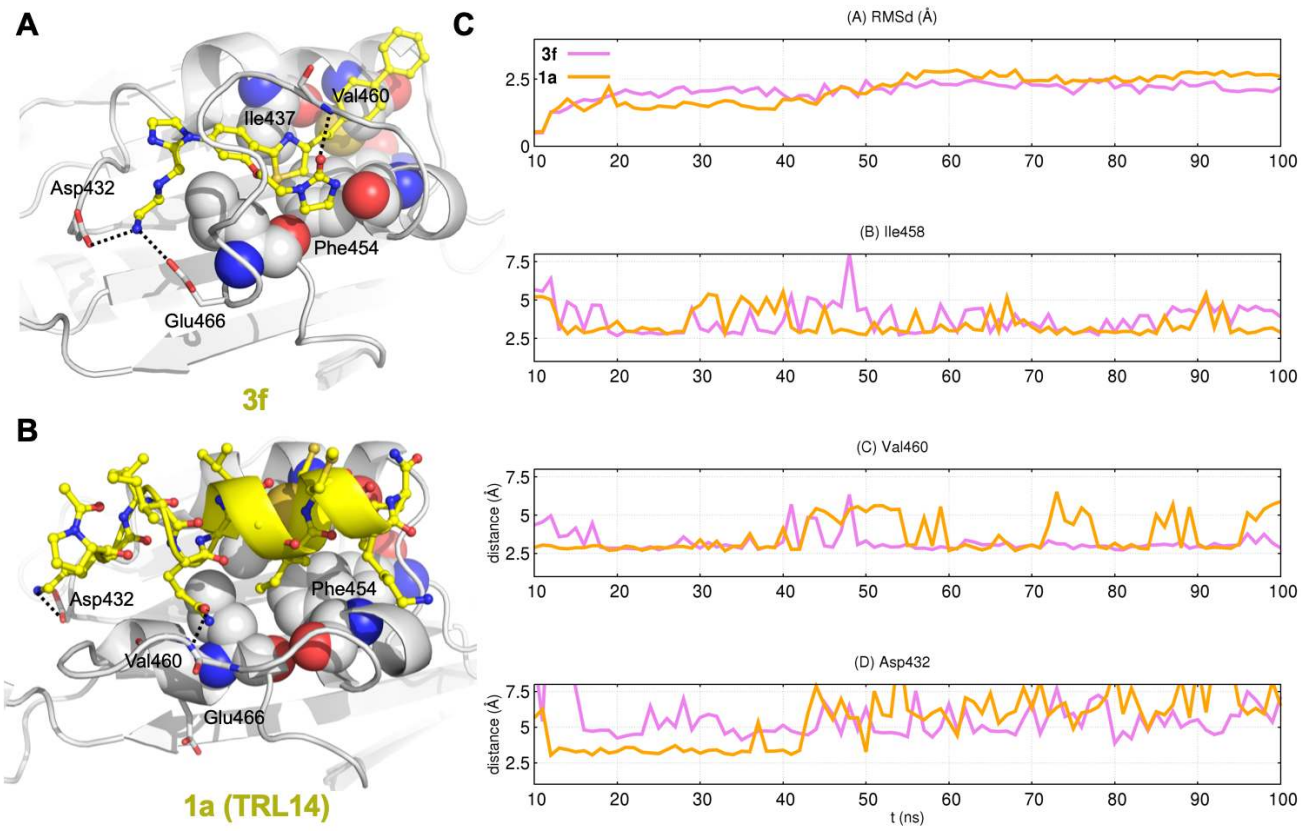

Figure 3. Comparative results from molecular dynamics (MD) simulations of *Li*-TryR:**1a** and *Li*-TryR:**3f** complexes. (**A**) Representative structure of **3f** (shown as sticks and balls; C atoms colored in yellow) bound at the dimerization interface of a *Li*-TryR monomer (C atoms colored in grey). (**B**) Representative structure of the complex formed between a *Li*-TryR monomer and peptide **1a** (TRL14) (**1a**) with a Lys at position 2 (P**K**IIQSVGICMKM, C atoms colored in yellow). (**C**) Evolution of the root-mean-square deviation (RMSd, Å) of bound **3f** or **1a** (top) and time evolution of the distances (Å) separating **3f** from the backbone oxygen of Ile458, backbone nitrogen of Val460 (middle) and the carboxylate oxygen of Asp432 (bottom) along 100 ns of unrestrained MD simulation.

Taken together, our results point to at least two different binding sites for the compounds studied here. One, as shown in the crystal structure solved, is at the active site and may contribute to binding and subsequent enzyme inhibition through direct competition with Try. A second one should be located at the dimerization interface but we have been unable to detect it so far by X-ray crystallography because the monomeric form of the enzyme is unstable and does not form good crystals and/or spoils existing ones. The results obtained for series **3** strongly suggest that the

presence of a bulky substituent at R_3 is highly relevant for binding to this second site and for the ligand to behave as a dimerization disruptor.

Antileishmanial activity in cell culture. All the compounds were tested against *L. infantum* axenic amastigotes and promastigotes using miltefosine and the R_9-conjugate of the prototype peptide as positive controls. Neither the pyrrolopyrimidine compounds **2a-i** nor the imidazole-phenyl-thiazole analogues **3a-d** exhibited any significant antileishmanial activity at the maximum concentration assayed (25 μM). On the contrary, the most potent Li-TryR inhibitors **3e** and **3f**, for which a modest dimer disruption activity was also observed *in vitro*, displayed potent leishmanicidal activity (Table 2). Significantly, the activity against amastigotes of peptidomimetic **3f** was found to be similar to that observed for our peptidic prototype and for the reference drug miltefosine. The toxicity against the human cell line THP-1 was also found to be similar between **3f** and the R_9-conjugated peptide **1** and only slightly higher than that observed for miltefosine.

Cell penetration of the antileishmanicidal imidazole-phenyl-thiazole compounds was demonstrated by direct visualization of their intrinsic fluorescence inside *L. infantum* promastigotes (Figure 4).

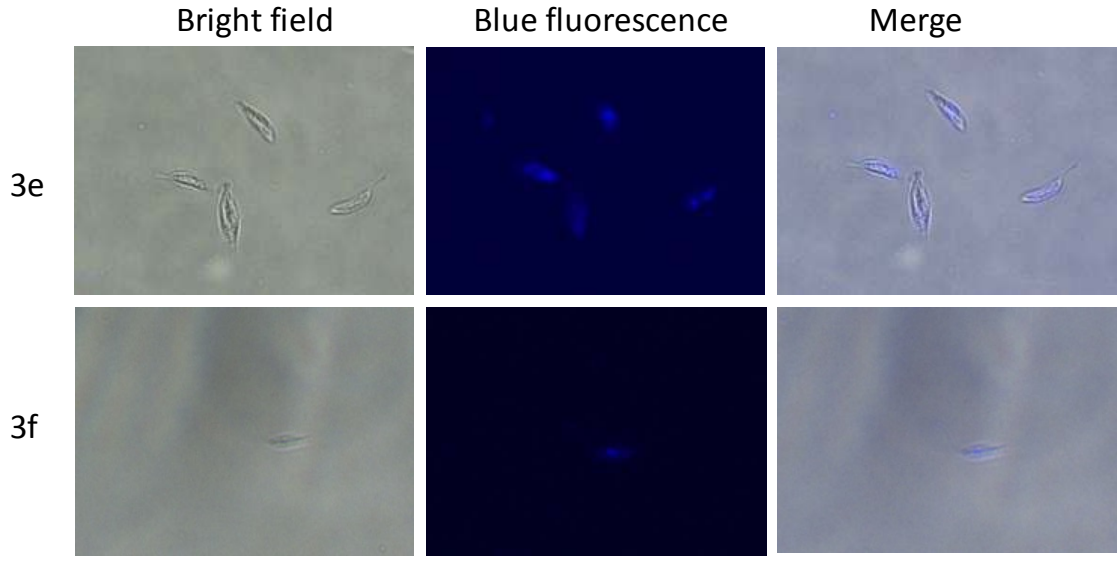

Figure 4. Fluorescence microscopy images of *L. infantum* promastigotes treated with 25 μM of compounds **3e** and **3f** for 1 h.

Compounds **3e** and **3f** were also able to cross the macrophage plasma and phagolysosomal membranes, as indicated by their capacity to decrease the parasite load in amastigote-infected THP-1 cells (EC_{50} values of 21.5 μM and 14.5 μM respectively).

A good correlation between the TryR inhibitory activity values and the *in cellulo* results is observed, which supports the idea that this enzyme may be the main molecular target of the imidazole-phenyl-thiazole analogues in *L. infantum* parasites.

Table 2: EC_{50} ± SEM values for the most active compounds **3e** and **3f** on *L. infantum* promastigotes, amastigotes and cytotoxic activity in THP-1 cells.[a]

Comp.	**R_3**	**EC_{50} promastigotes (μM)**	**EC_{50} amastigotes (μM)**	**EC_{50} THP-1 (μM)**
Miltefosine	/	47.6 ± 0.6	2 ± 0.1	29.9 ± 1.5
R_9-conjugated peptide **1**	/	4.6 ± 0.2	3.5 ± 0.9	12.6 ± 3.5
3e	$(CH_2)_2$-Naphthyl	12.8 ± 0.7	12.8 ± 1.3	26.5 ± 0.9
3f	$(CH_2)_2$-Biphenyl	5.3 ± 0.3	5.3 ± 0.2	14.2 ± 14.2

[a] EC_{50} = Half-maximal effective concentration. Results are representative of three independent experiments each performed in triplicate.

CONCLUSION

We believe that the development of drugs able to inhibit dimerization of functionally obligate homodimeric enzymes is an attractive goal. Recently, we succesfully developed peptide-based dimerization inhibitors of the homodimeric TryR from *L. infantum* that were derived from an α-helix located in the interfacial domain. However, conjugation to cell-penetrating peptides was required to kill the parasites in cell culture. With the aim of identifying small-molecule *Li*-TryR dimerization inhibitors with better drug-like properties, we then devised two α-helical proteomimetics, the pyrrolopyirimidine and the imidazo-phenyl-thiazole scaffolds, which we decorated with surrogates of the side-chains of key amino acids present in the prototype peptide. The pyrrolopyrimidine analogues behaved as moderate inhibitors of the oxidorreductase activity of *Li*-TryR but did not show any relevant enzyme disruption capacity and did not kill the parasites. The crystal structure of *Li*-TryR with pyrrolopyrimidine **2f** revealed that this compound binds to the "mepacrine binding site" of the large active site and represents a novel class of bicyclic and heterocyclic TryR inhibitor. On the other hand, the use of the imidazo-phenyl-thiazole scaffold allowed us to identify **3e** and **3f** as the first non-peptidic *Li*-TryR dissociative inhibitors that display *in vitro* leishmanicidal activities similar to those of our previous peptide-based compounds. The nice correlation between enzyme inhibition and antileishmanial activity against both extra- and intracellular *L. infantum* forms suggests that the compounds probably act by inhibiting *Li*-TryR. Comparative MD simulations of compound **3f** and the linear peptide prototype **1a** each bound at the dimerization interface of a *Li*-TryR monomer provide support to the pharmacophore hypothesis that the presence of a bulky aromatic group is essential for the ability of these molecules to disrupt enzyme dimerization. Studies are currently underway on the more promising imidazo-phenyl-thiazole class of small molecules for further optimization and development in our search for novel and safer anti-leishmanial agents.

EXPERIMENTAL SECTION

Chemistry. Melting points were obtained on a Mettler Toledo M170 apparatus and are uncorrected. IR spectra were obtained on a Perkin-Elmer Spectrum One spectrophotometer. Microanalyses were obtained with a Heraeus CHN-O-RAPID instrument and the analytical results were within 0.4% of the theoretical values. Electrospray mass spectra were measured on a quadropole mass spectrometer equipped with an electrospray source (Hewlett Packard, LC/MS HP 1100). HRMS (EI+) was carried out in an Agilent 6520 Accurate-Mass Q-TOF LC/MS spectrometer using water/acetonitrile. Spectra were recorded with a Varian Inova-300 or Mercury 400 spectrometers operating at 300 MHz or at 400 MHz for ^{1}H NMR and at 75 MHz or at 100 MHz for ^{13}C NMR with Me_4Si as internal standard.

Analytical thin-layer chromatography (TLC) was performed on silica gel 60 F_{254} (Merck). Compounds were purified by: a) flash column chromatography with silica gel 60 (230-400 mesh) (Merck), b) preparative centrifugal circular thin layer chromatography (CCTLC) on a Chromatotron (Kiesegel 60 PF_{254} gipshaltig (Merck), layer thickness (1 mm), flow rate (5 mL/min), c) HPFC (High Performance Flash Chromatography) purification in an Isolera One system (Biotage®) (Claricep i-Series, Silica, 40g, 40-60μm, 60Å and KP-C18-HS 12g, 21 x 55mm) or d) semipreparative HPLC instrument.

Pyrrolopyrimidines **2a-i** were synthesized on solid phase manually on a 20-positions vacuum manifold (*Omega*) connected to a vacuum pump using 20-mL polypropylene plastic syringes (*Dubelcco*) with a preinserted frit and a Teflon stopcock to do the washings and remove the solvents and excess of the reagents. The reactions were stirred using an *IKA-100* orbital shaker. After cleavage, the acidic crudes were sedimented in Et_2O on a *Hettlich Universal* 320R centrifuge at 5000 rpm. All the crude and samples were lyophilized using mixtures water/acetonitrile on a Telstar 6-80 instrument. The monitoring of the reactions was performed by HPLC/MS through a HPLC-

waters 12695 connected to a Waters Micromass ZQ spectrometer. 5-6-5 imidazole-phenyl-thiazole **3a-f** were synthesized in solution phase.

The purity of the final products was checked by analytical RP-HPLC on an Agilent Infinity instrument equipped with a Diode Array and a C18 Sunfire column (4.6 mm x 150 mm, 3.5 μ m). As mobile phase, A:B mixtures were used, where A = 0.05% TFA water and B = acetonitrile. The purity was also determined to be > 95% by elemental analysis and/or HRMS.

Unless otherwise noted, analytical grade solvents and commercially available reagents were used without further purification. THF was dried by reflux over sodium/benzophenone. Fmoc-protected Rink Amide MBHA resin (0.56 mmol/g or 0.71 mmol/g loading) was purchased from *Iris Biotech* (Germany). Microwave reactions were performed using the Biotage Initiator 2.0 single-mode cavity instrument from Biotage (Uppsala). Experiments were carried out in sealed microwave process vials utilizing the standard absorbance level (400 W maximum irradiation power).

Synthesis of pyrrolopyrimidine-based proteomimetics 2a-i.

General procedure for the solid-phase synthesis of pyrrolopyrimidines 2a-h from the Boc protected peptoidyl resin 6. Rink amide MBHA resin 0.56 mmol/g loading (300 mg, 0.168 mmol) was swelled with DMF (2 mL). The Fmoc protecting group on the resin was removed by treating with 20% piperidine in DMF (1 x 1 min and 3 x 10 min). The resin was washed with DMF/DCM/DMF/DCM/DMF (4 x 0.5 min each time). A solution of bromoacetic acid (0.35 g, 2.52 mmol) and diisopropylcarbodiimide (DIC) (0.32 g, 2.52 mmol) in dry DMF (2 mL) was added to the resin and stirred at room temperature for 30 min. This process was repeated twice and the resin was drained and washed with DMF/DCM/DMF/DCM/DMF. Then, the resin **4** was reacted with *N*-Boc-1,4-butanediamine (0.63 mL, 3.36 mmol) in dry DMF (2 mL) for 3 h at room temperature. The resin **5** was treated again with bromoacetic acid and DIC in DMF (2 x 30 min) followed by treatment with 3-aminopropanamide (0.42 g, 3.36 mmol) and TEA (0.93 mL, 6.72 mmol) in dry DMSO (3.4 mL) for 2 h at room temperature. After washing and swelling the resin **6** was reacted

with a solution of the appropriate previously synthesized 2-alkylamine-4,6-(dichloro)pyrimidine-5-carbaldehyde **12a-g** or commercially available **12h** (5 equiv) with TEA (5 equiv) in dry THF (4 mL) at room temperature overnight. For dimethylamination and cyclization, the resins **14a-h** were treated first with a 2 M solution of dimethylamine in THF (1.68 mL, 3.36 mmol) and DIEA (0.57 mL, 3.36 mmol) in dry NMP (2 mL) in a pressure tube at 60 °C overnight. After washing and swelling, the resulting resins **15a-h** were reacted with DBU (0.3 mL, 3.36 mmol) in dry DMF (3 mL) in a pressure tube at 90 ºC overnight to give the pyrrolopyrimidine resins **16a-h**. After thorough washing (DMF/DCM/DMF/DCM) the final pyrrolopyrimidines **2a-h** were cleaved from the resin using an acidolitic cleavage cocktail (TFA:TIPS:H_2O 95:2.5:2.5) for 2 h at room temperature. The filtrates were precipitated from cold diethylether (50 mL), centrifuged at 5000 rpm (3 x 10 min) and lyophilized. The cleaved final products were purified by reverse phase chromatography in the Biotage® (from 0% initial of A to 100% final of A) or by semipreparative HPLC.

4-(N-(2-Amino-2-oxoethyl)-7-(3-amino-3-oxopropyl)-2-(sec-butylamino)-4-(dimethylamino)-7H-pyrrolo[2,3-d]pyrimidine-6-carboxamido)butan-1-aminium 2,2,2-trifluoroacetate **(2a).** According to the general procedure, the peptoidyl resin **6** was reacted with 2-(*sec*-butylamine)-4,6-dichloropyrimidine-5-carbaldehyde **12a** (135 mg, 0.588 mmol) and TEA in dry THF. After dimethylamination, cyclization and cleavage, the final crude was purified on the Biotage® to give 18 mg (22% yield) of **2a** (TFA salt) as a yellow amorphous solid. HPLC (2% to 30% of acetonitrile in 10 min): Rt = 5.58 min (>91% purity); ^{1}H NMR (400 MHz, DMSO-d_6, 90 ºC) δ (ppm): 7.68 (bs, 3H, N$\underline{H}_3^+$), 7.06 (bs, 4H, 2CON$\underline{H}_2$), 6.71 (s, 1H, Ar), 5.78 (bs, 1H, NH), 4.30 (t, *J* = 7.5 Hz, 2H, CH_2N_{pyr}), 4.09 (s, 2H, COC$\underline{H}_2$N), 3.93 (q, *J* = 6.5 Hz, 1H, CH), 3.47 (t, *J* = 7.1 Hz, 2H, C$\underline{H}_2$NH$_3^+$), 3.23 (s, 6H, 2CH_3N), 2.84 (t, *J* = 7.2 Hz, 2H, $CH_2C\underline{H}_2$NCO), 2.59-2.53 (m, 2H, C$\underline{H}_2$CONH$_2$), 1.73-1.54 (m, 4H, $NH_3^+CH_2C\underline{H}_2C\underline{H}_2$), 1.53-1.43 (m, 2H, C$\underline{H}_2CH_3$), 1.16 (d, *J* = 6.6 Hz, 3H, CHC$\underline{H}_3$), 0.90 (t, *J* = 7.4 Hz, 3H, $CH_2C\underline{H}_3$); ^{13}C NMR (125 MHz, DMSO-d_6, rt) δ (ppm): 172.3 (2$\underline{C}$ONH$_2$),

164.1 (2C), 158.1 (q, *J* = 31 Hz, $CF_3\underline{C}OO^-$), 157.6 (2C), 123.9 (C_{Ar}), 117.3 (q, *J* = 300 Hz, $\underline{C}F_3COO^-$), 104.9 (CH_{Ar}), 94.8 (C_{Ar}), 51.9 ($CO\underline{C}H_2N$), 47.7 (<u>C</u>H-NH), 45.9 ($\underline{C}H_2NH_3^+$), 38.7 ($CH_2\underline{C}H_2NCO$), 38.7 ($2\underline{C}H_2N_{pyr}$), 38.6 ($2\underline{C}H_3N$), 34.9 ($\underline{C}H_2CONH_2$), 29.1 ($\underline{C}H_2$-CH_3), 24.5 ($NH_3^+CH_2\underline{C}H_2\underline{C}H_2$), 20.3 ($\underline{C}H_3$-CH), 10.9 ($\underline{C}H_3$-$CH_2$); HRMS (ESI positive, *m/z*): calculated for $C_{22}H_{37}N_9O_3$ 475.3019; found 475.3018 (-0.16 ppm); Anal. Calcd. for $C_{22}H_{37}N_9O_3 \cdot 1.5$ TFA $\cdot$ 2 H_2O: C, 43.99; H, 6.28; N, 18.47. Found: C, 44.24; H, 6.27; N, 18.65.

4-(N-(2-Amino-2-oxoethyl)-7-(3-amino-3-oxopropyl)-4-(dimethylamino)-2-(isobutylamino)-7H-pyrrolo[2,3-d]pyrimidine-6-carboxamido)butan-1-aminium 2,2,2-trifluoroacetate **(2b).** Following the general procedure, the peptoidyl resin **6** was reacted with 2-(isobutylamine)-4,6-dichloropyrimidine-5-carbaldehyde **12b** (146 mg, 0.588 mmol) and TEA in dry THF. After dimethylamination, cyclization and cleavage, the final crude was purified on the Biotage® to give 18 mg (22% yield) of **2b** (TFA salt) as a yellow amorphous solid. HPLC (2% to 30% of acetonitrile in 10 min): Rt = 5.63 min. (>93% purity); ^{1}H NMR (400 MHz, DMSO-d_6, 90 ºC) δ (ppm): 7.68 (bs, 3H, $N\underline{H}_3^+$), 7.10 (bs, 4H, $2CON\underline{H}_2$), 6.70 (s, 1H, Ar), 4.28 (t, *J* = 7.3 Hz, 2H, CH_2-$C\underline{H}_2N_{pyr}$), 4.06 (s, 2H, $COC\underline{H}_2N$), 3.44 (t, *J* = 7.2 Hz, 2H, $C\underline{H}_2NH_3^+$), 3.22 (s, 6H, $2C\underline{H}_3N$), 3.14 (d, *J* = 6.7 Hz, 2H, $CHC\underline{H}_2NH$), 2.82 (t, *J* = 7.2 Hz, 2H, $CH_2C\underline{H}_2NCO$), 2.53 (t, *J* = 7.5 Hz, 2H, $C\underline{H}_2CONH_2$), 1.89 (hept, *J* = 6.7 Hz, 1H, C<u>H</u>), 1.75-1.45 (m, 4H, $NH_3^+CH_2C\underline{H}_2C\underline{H}_2$), 0.89 (d, *J* = 6.7 Hz, 6H, $2C\underline{H}_3$); ^{13}C NMR (125 MHz, DMSO-d_6, rt) δ (ppm): 172.3 ($2CONH_2$), 164.0 (2C), 158.2 (q, *J* = 31 Hz, $CF_3\underline{C}OO^-$), 157.8 (2C), 124.2 (C_{Ar}), 117.2 (q, *J* = 300 Hz, $\underline{C}F_3COO^-$), 105.1 (CH_{Ar}), 94.7 (C_{Ar}), 51.9 ($CO\underline{C}H_2N$), 49.1 ($CH\underline{C}H_2NH$), 46.3 ($\underline{C}H_2NH_3^+$), 39.1 ($CH_2\underline{C}H_2NCO$), 39.0 ($2\underline{C}H_3$), 38.9 (CH_2-$\underline{C}H_2$-N_{pyr}), 34.8 ($\underline{C}H_2CONH_2$), 28.1 (CH), 24.5 ($NH_3^+CH_2\underline{C}H_2\underline{C}H_2$), 20.8 ($2\underline{C}H_3$); HRMS (ESI positive, *m/z*): calculated for $C_{22}H_{37}N_9O_3$ 475.3019; found 475.3013 (-1.37 ppm); Anal. Calcd. for $C_{22}H_{37}N_9O_3 \cdot 1.5$ TFA $\cdot$ 2 H_2O: C, 43.99; H, 6.28; N, 18.47. Found: C, 44.12; H, 6.31; N, 18.30.

4-(N-(2-Amino-2-oxoethyl)-7-(3-amino-3-oxopropyl)-2-(benzylamino)-4-(dimethylamino)-7H-pyrrolo[2,3-d]pyrimidine-6-carboxamido)butan-1-aminium 2,2,2-trifluoroacetate **(2c).** The peptoidyl resin **6** was reacted with 2-(benzylamine)-4,6-dichloropyrimidine-5-carbaldehyde **12c** (166 mg, 0.588 mmol) and TEA in dry THF following the general procedure. After dimethylamination, cyclization and cleavage, the final crude was purified on the Biotage® to give 18 mg (21% yield) of **2c** (TFA salt) as a yellow amorphous solid. HPLC (2% to 30% of acetonitrile in 10 min): Rt = 5.88 min (>95% purity); ^{1}H NMR (400 MHz, DMSO-d_6, 90 ºC) δ (ppm): 8.29 (bs, 3H, $N\underline{H}_3^+$), 7.38 (d, *J* = 7.5 Hz, 2H, Ar), 7.27 (t, *J* = 7.5 Hz, 2H, Ar), 7.18 (t, *J* = 7.3 Hz, 1H, Ar), 6.69 (s, 1H, $C\underline{H}_{Ar(pyr)}$), 6.59 (t, *J* = 6.3 Hz, 1H, NH), 4.50 (d, *J* = 6.1 Hz, 2H, $C\underline{H}_2NH$), 4.30 (t, *J* = 7.5 Hz, 2H, CH_2N_{pyr}), 4.08 (s, 2H, $COC\underline{H}_2N$), 3.46 (t, *J* = 7.2 Hz, 2H, $C\underline{H}_2NH_3^+$), 3.20 (s, 6H, $2C\underline{H}_3N$), 2.78 (t, *J* = 7.2 Hz, 2H, $CH_2C\underline{H}_2NCO$), 2.54 (t, *J* = 7.6, 2H, $C\underline{H}_2CONH_2$), 1.73-1.33 (m, 4H, $NH_3^+CH_2C\underline{H}_2C\underline{H}_2$); ^{13}C NMR (125 MHz, DMSO-d_6, rt) δ (ppm): 172.4 ($2CONH_2$), 164.2 (2C), 159.0 (C), 158.0 (q, *J* = 31 Hz, $CF_3\underline{C}OO^-$), 157.8 (C), 141.7 (C_{benz}), 128.0 ($2CH_{benz}$), 127.6 (CH_{benz}), 126.3 ($2\underline{C}H_{benz}$), 123.9 (C_{Ar}), 117.3 (q, *J* = 300 Hz, $\underline{C}F_3COO^-$), 104.7 (CH_{Ar}), 95.1 (C_{Ar}), 51.9 ($CO\underline{C}H_2N$), 45.8 ($\underline{C}H_2NH$), 44.6 ($CH_2NH_3^+$), 38.7 ($CH_2\underline{C}H_2NCO$), 38.6 (CH_2N_{pyr}), 38.5 ($2CH_3N$), 34.9 ($\underline{C}H_2CONH_2$), 24.7 ($NH_3^+CH_2\underline{C}H_2\underline{C}H_2$); HRMS (ESI positive, *m/z*): calculated for $C_{25}H_{35}N_9O_3$ 509.2863; found 509.2864 (0.17 ppm); Anal. Calcd. for $C_{25}H_{35}N_9O_3 \cdot 1.2$ TFA $\cdot 2.6$ H_2O: C, 47.47; H, 6.02; N, 18.18. Found: C, 47.04; H, 6.05; N, 18.61.

4-(N-(2-Amino-2-oxoethyl)-7-(3-amino-3-oxopropyl)-4-(dimethylamino)-2-(phenethylamino)-7H-pyrrolo[2,3-d]pyrimidine-6-carboxamido)butan-1-aminium 2,2,2-trifluoroacetate **(2d).** According to the general procedure, the peptoidyl resin **6** was reacted with 2-(phenylethylamine)-4,6-dichloropyrimidine-5-carbaldehyde **12d** (174 mg, 0.588 mmol) and TEA in dry THF. After dimethylamination, cyclization and cleavage, the final crude was purified on the Biotage® to give 7 mg (10% yield) of **2d** (TFA salt) as a yellow amorphous solid. HPLC (2% to 30% of acetonitrile in 10 min): Rt = 7.52 min. (>95% purity); ^{1}H NMR (400 MHz, DMSO-d_6, 90 ºC) δ (ppm): 8.29 (bs,

1H, NH), 7.35-7.25 (m, 5HAr), 7.23-7.15 (m, 1HAr), 6.70 (s, 1HArpyr), 6.01 (bs, 1H, NH), 4.33 (t, *J* = 7.4 Hz, 1H, C$\underline{H_2}$-Npyr), 4.08 (s, 1H, N-C$\underline{H_2}$-$CONH_2$), 3.54 (q, *J* = 6.7 Hz, 2H, C$\underline{H_2}$-NH), 3.49-3.45 (m, 2H, NH_2-C$\underline{H_2}$-CH_2), 3.24 (s, 6H, $2CH_3$-N), 2.92-2.88 (M, 2H, CH_2-Ph), 2.70-2.67 (m, 2H, CH_2-NCO), 2.59-2.56 (m, 2H, CH_2-$CONH_2$), 1.70-1.63 (m, 2H, C$\underline{H_2}$-CH_2-N), 1.50-1.42 (m, 2H, C$\underline{H_2}$-CH_2-NH_2); ^{13}C NMR (125 MHz, DMSO-d_6, rt) δ (ppm): 26.2 ($2CH_2$), 35.3 (C$\underline{H_2}$-$CONH_2$), 36.2 (C$\underline{H_2}$-Ph), 38.7 (C$\underline{H_2}$-N_{pyr}), 38.9 ($2C\underline{H_3}$-N), 39.4 (CH_2-C$\underline{H_2}$-N), 43.6 (C$\underline{H_2}$-NH_2), 95.5 (C_{Ar}), 105.1 (CH_{Arpyr}), 117.2 (q, *J* = 300 Hz, C$\underline{F_3}$$COO^-$), 124.4 ($C_{Ar}$), 126.3 ($CH_{benz}$), 128.8 ($2CH_{benz}$), 129.1 ($2CH_{benz}$), 140.7 ($C_{benz}$), 154.7 (C), 158.4 (q, *J* = 31 Hz, CF_3C$\underline{O}O^-$), 159.5 (C), 164.6 (C), 172.8 ($2CONH_2$); HRMS (ESI positive, *m/z*): calculated for $C_{26}H_{37}N_9O_3$ 523.30194; found 523.30215 (0.4 ppm).

4-(N-(2-amino-2-oxoethyl)-7-(3-amino-3-oxopropyl)-4-(dimethylamino)-2-((3-phenylpropyl)amino)-7H-pyrrolo[2,3-d]pyrimidine-6-carboxamido)butan-1-aminium 2,2,2-trifluoroacetate **(2e).** Following the general procedure, the peptoidyl resin **6** was reacted with 2-(phenylpropylamine)-4,6-dichloropyrimidine-5-carbaldehyde **12e** (182 mg, 0.588 mmol) and TEA in dry THF. After dimethylamination, cyclization and cleavage, the final crude was purified on the Biotage® to give 20 mg (22% yield) of **2e** (TFA salt) as a yellow amorphous solid. HPLC (2% to 30% of acetonitrile in 10 min): Rt = 5.52 min (>95% purity); ^{1}H NMR (400 MHz, DMSO-d_6, 90 °C) δ (ppm): 7.70 (bs, 1H, NH_3^+), 7.52 (bs, NHCO), 7.33 (bs, NHCO), 7.27-7.23 (m, 5HAr), 6.85 (bs, NHCO), 6.77 (bs, NHCO), 4.25 (t, *J* = 7.0 Hz, 2H, CH_2-N_{pyr}), 4.04 (s, 2H, N-C$\underline{H_2}$-$CONH_2$), 3.50-3.40 (m, 2H, CH_2-NH), 3.32 - 3.25 (m, 2H, C$\underline{H_2}$-NH_3), 3.22 (s, 6H, $2CH_3$-N), 2.84-2.74 (m, 2H, CH_2), 2.62 (t, *J* = 7.6 Hz, 2H, CH_2-NCO), 2.52 (t, *J* = 7.1 Hz, 2H, CH_2-$CONH_2$), 1.87-1.80 (m, 2H, CH_2), 1.65-1.40 (m, 4H, $2CH_2$); HRMS (ESI positive, *m/z*): calculated for $C_{27}H_{41}N_9O_3$ 527.33324; found 527.33265 (-1.1 ppm).

4-(N-(2-Amino-2-oxoethyl)-7-(3-amino-3-oxopropyl)-4-(dimethylamino)-2-((2-(naphthalen-2-yl)ethyl)amino)-7H-pyrrolo[2,3-d]pyrimidine-6-carboxamido)butan-1-aminium 2,2,2-trifluoroacetate **(2f).** The peptoidyl resin **6** was reacted with 2-(naphthylethylamine)-4,6-dichloropyrimidine-5-carbaldehyde **12f** (203 mg, 0.588 mmol) and TEA in dry THF according to the general procedure. After dimethylamination, cyclization and cleavage, the final crude was purified on the Biotage® to give 10 mg (11% yield) of **2f** (TFA salt) as a yellow amorphous solid. HPLC (2% to 30% of acetonitrile in 10 min): Rt = 5.85 min. (>98% purity); ^{1}H NMR (400 MHz, DMSO-d_6, 90 °C) δ (ppm): 7.89 (bs, 3H, NH_3^+), 7.75-7.40 (m, 7HAr), 6.72 (s, $1H_{Arpyr}$), 6.10 (bs, 1H, NH), 4.35 (t, *J* = 7.3 Hz, 1H, $C\underline{H}_2$-Npyr), 4.10 (s, 1H, N-$C\underline{H}_2$-$CONH_2$), 3.69-3.61 (m, 2H, $C\underline{H}_2$-NH), 3.49-3.40 (m, 2H, NH_2-$C\underline{H}_2$-CH_2), 3.24 (s, 6H, $2CH_3$-N), 2.89-2.79 (m, 4H, $2CH_2$), 2.64-2.57 (m, 2H, CH_2-$CONH_2$), 1.72-1.58 (m, 4H, $2CH_2$); HRMS (ESI positive, *m/z*): calculated for $C_{30}H_{39}N_9O_3$ 573.31759; found 573.31955 (3.43 ppm).

4-(2-(([1,1'-Biphenyl]-4-ylmethyl)amino)-N-(2-amino-2-oxoethyl)-7-(3-amino-3-oxopropyl)-4-(dimethylamino)-7H-pyrrolo[2,3-d]pyrimidine-6-carboxamido)butan-1-aminium 2,2,2-trifluoroacetate **(2g).** The peptoidyl resin **6** was reacted with 2-(([1,1'-biphenyl]-4-ylmethyl)amino)-4,6-(dichloro)pyrimidine-5-carbaldehyde **12g** (210 mg, 0.588 mmol) and TEA in dry THF following the general procedure. After dimethylamination, cyclization and cleavage, the final crude was purified on the Biotage® to give 28 mg (29% yield) of **2g** (TFA salt) as a white amorphous solid. HPLC (2% to 30% of acetonitrile in 10 min): Rt = 6.22 min. (>92% purity); ^{1}H NMR (400 MHz, DMSO-d_6, 90 °C) δ (ppm): 7.74 (bs, 3H, NH_3^+), 7.64-7.56 (m, 4HAr), 7.51-7.40 (m, 5H, Ar), 6.76 (s, $1H_{Arpyr}$), 4.58 (s, 1H, N-$C\underline{H}_2$-$CONH_2$), 4.33 (t, *J* = 7.4 Hz, 1H, $C\underline{H}_2$-Npyr), 4.10 (s, 1H, N-$C\underline{H}_2$-$CONH_2$), 4.02-3.68 (m, 2H, $C\underline{H}_2$-NH), 3.47 (t, *J* = 7.2 Hz, 1H, $C\underline{H}_2$-Npyr), 2.88-2.78 (m, 4H, $2CH_2$), 2.57 (dd, *J* = 8.2, 6.6 Hz, 2H, CH_2-$CONH_2$), 1.72-1.50 (m, 4H, $2CH_2$); ^{13}C NMR (125 MHz, DMSO-d_6, rt) δ (ppm): 24.4 (CH_2), 24.6 (CH_2), 31.7 ($\underline{C}H_2$-$CONH_2$), 34.7 ($\underline{C}H_2$-$CONH_2$), 37.7 ($\underline{C}H_2$-N_{pyr}), 38.4 ($2\underline{C}H_3$-N), 38.5 (CH_2-$\underline{C}H_2$-N), 45.7 ($\underline{C}H_2$-NH_2), 86.5 (CH_2-NH),

115.8 (C_{Ar}), 118.2 (C_{Ar}), 126.5 (CH_{Ar}), 126.6 (CH_{Ar}), 127.3 (C_{Ar}), 128.3 (C_{Ar}), 128.9 (CH_{Ar}), 138.6 (C_{Ar}), 140.0 (C_{Ar}), 158.2 (q, *J* = 31 Hz, $CF_3\underline{C}OO^-$), 165.4 (C_{Ar}), 169.4 (C_{Ar}), 169.6 ($CONH_2$), 172.2 ($CONH_2$); HRMS (ESI positive, *m/z*): calculated for $C_{31}H_{39}N_9O_3$ 585.3176; found 585.3170 (-1.07 ppm).

4-(N-(2-Amino-2-oxoethyl)-7-(3-amino-3-oxopropyl)-4-(dimethylamino)-2-(pyrrolidin-1-yl)-7H-pyrrolo[2,3-d]pyrimidine-6-carboxamido)butan-1-aminium 2,2,2-trifluoroacetate **(2h).** Following the general procedure, the peptoidyl resin **6** was reacted with commercially available 4,6-dichloro-2-(pyrrolidin-1-yl)pyrimidine-5-carbaldehyde **12h** (207 mg, 0.588 mmol) and TEA in dry THF. After dimethylamination, cyclization and cleavage, the final crude was purified on the Biotage to give 45 mg (57% yield) of **2h** (TFA salt) as a yellow amorphous solid. HPLC (2% to 100% of acetonitrile in 20 min): Rt = 3.87 min. (>99% purity); ^{1}H NMR (400 MHz, DMSO-d_6, 90 ºC) δ (ppm): 7.71 (bs, 3H, $N\underline{H}_3^+$), 7.06 (bs, 4H, $2CON\underline{H}_2$), 6.73 (s, 1H, Ar), 4.33 (t, *J* = 7.2 Hz, 2H, $C\underline{H}_2N_{pyr}$), 4.09 (s, 2H, $COC\underline{H}_2NCO$), 3.50-3.57 (m, 4H, $2\underline{C}H_2N_{pyrrolidine}$), 3.48 (t, *J* = 7.1 Hz, 2H, $C\underline{H}_2NH_3^+$), 3.25 (s, 6H, $2C\underline{H}_3N$), 2.84 (t, *J* = 7.2 Hz, 2H, $CH_2C\underline{H}_2NCO$), 2.59 (t, *J* = 7.2 Hz, 2H, $C\underline{H}_2CONH_2$), 1.97-1.85 (m, 4H, $2C\underline{H}_{2\ pyrrolidine}$), 1.82-1.46 (m, 4H, $NH_3^+CH_2C\underline{H}_2C\underline{H}_2$); ^{13}C NMR (101 MHz, DMSO-d_6, rt) δ (ppm): 172.8 ($2\underline{C}ONH_2$), 164.0 (2C), 158.1 (q, *J* = 32 Hz, $CF_3\underline{C}OO^-$), 157.4 (2C), 124.2 (C_{Ar}), 117.1 (q, *J* = 301 Hz, $\underline{C}F_3COO^-$), 104.3 (CH_{Ar}), 94.5 (C_{Ar}), 46.3 ($2CH_2N_{pyrrolidine}$), 38.9 ($CH_2\underline{C}H_2NCO$), 38.6 (CH_2N_{pyr}), 38.5 ($2CH_3N$), 34.8 ($\underline{C}H_2CONH_2$), 25.0 ($2\underline{C}H_{2pyrrolidine}$), 24.5 ($NH_3^+CH_2\underline{C}H_2\underline{C}H_2$); HRMS (ESI positive, *m/z*): calculated for $C_{22}H_{35}N_9O_3$ 473.2863; found 473.2869 (1.33 ppm).

Solid-phase synthesis of pyrrolopyrimidine 2i from Alloc protected peptoidyl resin 6'.

1-(4-(N-(2-Amino-2-oxoethyl)-7-(3-amino-3-oxopropyl)-4-(dimethylamino)-2-(2-(naphthalen-2-yl)ethyl)-7H-pyrrolo[2,3-d]pyrimidine-6-carboxamido)butyl)guanidinium 2,2,2-trifluoroacetate **(2i).** Following the general procedure for the synthesis of pyrrolopyrimidines **2a-h**, Rink amide

MBHA resin 0.71 mmol/g loading (450 mg, 0.32 mmol) was swelled with DMF (2 mL). The Fmoc protecting group on the resin was removed by treating with 20% piperidine in DMF (1 x 1 min and 3 x 10 min). The resin was washed (4 x 0.5 min each time, DMF/DCM/DMF/DCM/DMF). A solution of bromoacetic acid (0.67 g, 4.8 mmol) and diisopropylcarbodiimide (DIC) (0.74 g, 4.8 mmol) in dry DMF (2 mL) was added to the resin and stirred at room temperature for 30 min. This process was repeated twice and the resin was drained and washed with DMF/DCM/DMF/DCM/DMF. Then, the resin **4** was reacted with *N*-Alloc-1,4-butanediamine[45] (277 mg, 1.6 mmol) in dry DMF (2 mL) for 2 h at room temperature. The resulting resin was treated again with bromoacetic acid and DIC in DMF (2 x 30 min) followed by treatment with 3-aminopropanamide (0.40 g, 3.2 mmol) and TEA (0.89 mL, 6.4 mmol) in dry DMSO (3 mL) for 2 h at room temperature. After washing and swelling the Alloc protected peptoidyl resin **6'** was treated with a solution of **12f** (573 mg, 1.6 mmol) and TEA (0.22 mL, 1.6 mmol) in dry THF (4 mL) at room temperature overnight. For dimethylamination and cyclization, the resin **14'f** was reacted first with a 2 M solution of dimethylamine in THF (3.2 mL, 6.4 mmol) and DIEA (1.09 mL, 6.4 mmol) in dry NMP (2 mL) in a pressure tube at 60 °C overnight. After washing and swelling the resin was reacted with DBU (0.6 mL, 6.4 mmol) in dry DMF (3 mL) in a pressure tube at 90 ºC overnight. After washing and swelling the resin, Alloc deprotection was performed by treatment of the resin with $Pd(PPh_3)_4$ (92 mg, 0.08 mmol) and $PhSiH_3$ (0.95 mL, 7.68 mmol) in dry DCM at room temperature (2 x 1 h). Once the amino group was deprotected, the guanilidation reaction was carried out by reaction of the resin with 1,3-Di-Boc-2-(trifluoromethylsulfonyl)guanidine (626 mg, 1.6 mmol) and TEA (0.22 mL, 1.6 mmol) in dry DCM at room temperature for 5 h.[46] After thorough washing (DMF/DCM/DMF/DCM) the final pyrrolopyrimidine **2i** was cleaved from the resin using an acidolitic cleavage cocktail (TFA:TIPS:H_2O 95:2.5:2.5) for 2 h at room temperature. The filtrate was precipitated from cold diethylether (50 mL), centrifuged at 5000 rpm (3 x 10 min) and lyophilized. The cleaved final product was purified by reverse phase chromatography in the

Biotage® (from 0% initial of A to 100% final of A) to give 3.8 mg (2% yield) of the desired pyrrolopyrimidine **2i** as a yellow amorphous solid. HPLC (2% to 30% of acetonitrile in 10 min): Rt = 6.14 min (>98% purity); ^{1}H NMR (400 MHz, DMSO-d_6, 90 °C) δ (ppm): 7.88-7.81 (m, 2H, Ar), 7.76 (s, 1H, Ar), 7.54-7.41 (m, 3H, Ar), 7.38 (t, *J* = 5.7 Hz, 1H, Ar), 6.92 (bs, 3H, NH_3^+), 6.75 (s, $1H_{Arpyr}$), 4.35 (t, *J* = 7.3 Hz, 2H, C$\underline{H_2}$-Npyr), 4.10 (s, 2H, N-C$\underline{H_2}$-$CONH_2$), 3.72-3.60 (m, 2H, C$\underline{H_2}$-NH), 3.53-3.42 (m, 2H, NH_2-C$\underline{H_2}$-CH_2), 3.26 (s, 6H, $2CH_3$-N), 2.62 (t, *J* = 7.4 Hz, 2H, CH_2-$CONH_2$), 1.66 (quin, *J* = 7.2 Hz, 2H, CH_2), 1.53 (quin, *J* = 7.2 Hz, 2H, CH_2); ^{13}C NMR (125 MHz, DMSO-d_6, rt) δ (ppm): 172.5 ($\underline{C}ONH_2$), 172.3 ($\underline{C}ONH_2$), 164.0 (2C), 157.8 (q, *J* = 32 Hz, $CF_3\underline{C}OO^-$), 156.7 (C), 137.8 (C_{Ar}), 133.2 (C_{Ar}), 131.6 (C_{Ar}), 127.7 (CH_{Ar}), 127.6 (CH_{Ar}), 127.5 (C_{Ar}), 127.4 (CH_{Ar}), 127.3 (CH_{Ar}), 127.3 (C_{Ar}), 126.6 (CH_{Ar}), 126.6 (C_{Ar}), 125.9 (CH_{Ar}), 125.2 (CH_{Ar}), 95.0 (C_{Ar}), 42.9 ($CH_2N_{pyrrolidine}$), 40.6 (CH_2NCO), 35.8 ($\underline{C}H_2CONH_2$), 34.8 ($\underline{C}H_2CONH_2$), 33.9 (CH_2Napht), 26.0 ($2\underline{C}H_{2pyrrolidine}$), 23.3 ($NH_3^+CH_2\underline{C}H_2\underline{C}H_2$); HRMS (ESI positive, *m/z*): calculated for $C_{31}H_{41}N_{11}O_3$ 615.33938; found 615.33711 (-3.7 ppm).

Synthesis of 5-6-5 imidazole-phenyl-thiazole-based proteomimetics 3a-f

4-Iodo-2-(2-(2-oxoimidazolidinyl)ethoxy)benzonitrile **(22)**. To a solution of 1-(2-hydroxyethyl)imidazolidin-2-one (416 mg, 3.04 mmol) and 4-iodo-2-fluoro-benzonitrile **21** (500 mg, 2.02 mmol) in dry THF (40 mL), was added KHMDS 0,5 M in toluene (7.5 ml, 3.75 mmol) at 0 °C. The reaction mixture was stirred at room temperature overnight and the solvent was evaporated to dryness. The residue was dissolved in DCM (50 mL) and washed with HCl (3 x 30 mL). The aqueous phases were extracted with DCM (2 x 50 mL) and the combined organic phases were washed with brine (50 mL), dried (Na_2SO_4), filtered and evaporated to dryness. The residue was purified by flash column chromatography (DCM/MeOH, 9.75 : 0.25) to yield 420 mg (83% yield) of **22** as a yellow solid. Mp: 160-163 °C ; IR (KBr), ν (cm^{-1}): 3263 (N-H st), 2225 (C≡N st), 1695 (C=O st) ; ^{1}H NMR ($CDCl_3$, 300 MHz) δ (ppm): 7.33 (d, *J* = 8.2 Hz, 1H, Ar), 7.26 (s,

1H, Ar), 7.18 (d, *J* = 8.0 Hz, 1H, Ar), 4.70 (bs, 1H, NHCON), 4.14 (t, *J* = 4.9 Hz, 2H, $OC\underline{H_2}CH_2$), 3.71 (dd, *J* = 9.1, 6.6 Hz, 2H, $C\underline{H_2}CH_2NHCON$), 3.58 (t, *J* = 4.8 Hz, 2H, $OCH_2C\underline{H_2}$), 3.38 (t, *J* = 8.0 Hz, 2H, $CH_2C\underline{H_2}NHCON$); ^{13}C NMR ($CDCl_3$, 75 MHz) δ (ppm): 162.8 (NHCON), 160.2 (OC_{Ar}), 134.3 (CH_{Ar}), 130.7 (C_{Ar}), 121.9 (CH_{Ar}), 116.0 (CH_{Ar}), 101.7 (CN), 101.2 (C_{Ar}), 69.5 ($O\underline{C}H_2$), 47.5 ($\underline{C}H_2CH_2NHCON$), 43.2 ($OCH_2\underline{C}H_2$), 38.6 ($CH_2\underline{C}H_2NHCON$); MS (ESI, positive) *m/z*: 715.0 $[2M+H]^+$, 380.0 $[M+Na]^+$, 358.0 $[M+H]^+$

tert-Butyl (2-(((1-(4-cyano-3-(2-(2-oxoimidazolidin-1-yl)ethoxy)phenyl)-1H-imidazol-2-yl)methyl)amino)ethyl)carbamate **(25)**. A microwave vial (10 mL) was loaded with a solution of iodoarene **22** (100 mg, 0.28 mmol), imidazole **24** (135 mg, 0.56 mmol) and Cs_2CO_3 (183 mg, 0.56 mmol) in dry DMSO (3 mL) and was gently bubbled with argon. Then, *N,N*-dimethylglycine (2.9 mg, 0.03 mmol) and Cu_2O (cat) were added and the vial was sealed. The reaction mixture was heated at 85 °C (irradiation power 50 W) using microwave radiation for 2 h. The coupling reaction was repeated 3 times. Water was added (75 mL) and the reaction mixture was extracted with DCM (3 x 50 mL). The organic layers were combined, dried (Na_2SO_4), filtered and evaporated to dryness. The residue was purified by flash column chromatography (DCM/MeOH, 9 : 1) to yield 114 mg (87% yield) of **25** as a colourless oil. ^1H NMR (CD_3OD, 300 MHz) δ (ppm): 7.80 (d, *J* = 8.2 Hz, 1H, Ar), 7.62 (d, *J* = 1.8 Hz, 1H, Ar), 7.45 - 7.35 (m, 1H, Ar), 7.30 (dd, *J* = 8.2 Hz, 1.8 Hz, 1H, Ar), 7.14 - 7.05 (m, 1H, Ar), 4.34 (t, *J* = 5.1 Hz, 2H, $OC\underline{H_2}CH_2$), 3.89 - 3.80 (m, 2H, $ImC\underline{H_2}NH$), 3.76 (dd, *J* = 9.1, 7.0 Hz, 2H, $C\underline{H_2}CH_2NHCON$), 3.63 (t, *J* = 5.1 Hz, 2H, $OCH_2C\underline{H_2}$), 3.42 (dd, *J* = 9.5, 6.8 Hz, 2H, $CH_2C\underline{H_2}NHCON$), 3.15 - 3.10 (m, 2H, $CH_2C\underline{H_2}NHBoc$), 2.70 - 2.60 (m, 2H, $C\underline{H_2}CH_2NHBoc$), 1.42 (s, 9H, CH_3); ^{13}C NMR (CD_3OD, 75 MHz) δ (ppm): 165.1 (NHCON), 162.7 (OC_{Ar}), 158.5 (NHCOO), 147.6 (C_{Ar}), 144.0 (C_{Ar}), 135.9 (CH_{Ar}), 128.7 (CH_{Ar}), 122.6 (CH_{Im}), 122.6 (CH_{Im}), 119.1 (C_{Ar}), 116.6 (CN), 111.3 (CH_{Ar}), 102.5 (C_{Ar}), 80.1 ($O\underline{C}(CH_3)_3$), 70.0 (OCH_2), 49.6 ($\underline{C}H_2CH_2NHCON$), 48.0 ($OCH_2\underline{C}H_2$), 45.7 ($ImCH_2N$), 43.9 ($\underline{C}H_2CH_2NHBoc$), 41.2

($CH_2\underline{C}H_2NHCON$), 39.4 ($CH_2\underline{C}H_2NHBoc$), 28.8 ($CH_3$); HRMS (ESI positive, *m/z*): calculated for $C_{23}H_{31}N_7O_4$ 469.2438; found 469.2452 (3.02 ppm)

tert-Butyl (2-((tert-butoxycarbonyl)amino)ethyl)((1-(4-cyano-3-(2-(2-oxoimidazolidin-1-yl)ethoxy)phenyl)-1H-imidazol-2-yl)methyl)carbamate **(26)**. To a solution of compound **25** (100 mg, 0.214 mmol) and TEA (40 µl, 0.32 mmol) in MeOH (20 mL), Boc_2O (80 µl, 0.32 mmol) was added drop-wise. The reaction mixture was stirred at room temperature for 4 h and the solvent was removed at reduced pressure. The residue was dissolved in DCM (25 mL) and washed with water (2 x 20 mL). The organic layer was dried (Na_2SO_4), filtered and evaporated to dryness. The residue was purified by flash column chromatography (DCM/MeOH, 9.25 : 0.75) to give 112 mg (92% yield) of **26** as a colourless oil. ^{1}H NMR (CD_3OD, 300 MHz) δ (ppm): 7.81 - 7.71 (m, 1H, Ar), 7.46 - 7.36 (m, 1H, Ar), 7.32 (s, 1H, Ar), 7.12 (dd, *J* = 8.2, 1.8 Hz, 1H, Ar), 7.07 (s, 1H, Ar), 4.75 - 4.65 (m, 2H, $Im\underline{CH_2}N$), 4.39 - 4.31 (m, 2H, $OC\underline{H_2}CH_2$), 3.76 (dd, *J* = 8.9, 6.8 Hz, 2H, $C\underline{H_2}CH_2NHCON$), 3.62 (t, *J* = 5.2 Hz, 2H, $OCH_2C\underline{H_2}$), 3.42 (dd, *J* = 9.0, 7.0 Hz, 2H, $CH_2C\underline{H_2}NHCON$), 3.15 - 3.00 (m, 4H, $C\underline{H_2}C\underline{H_2}NHBoc$), 1.39 (s, 9H, CH_3), 1.34 (s, 9H, CH_3); ^{13}C NMR (CD_3OD, 75 MHz) δ (ppm): 165.4 (NHCON), 163.0 (OC_{Ar}), 158.6 (NHCOO), 156.9 (NHCOO), 146.4 (C_{Ar}), 144.1 (C_{Ar}), 136.1 (CH_{Ar}), 129.1 (CH_{Ar}), 123.8 (CH_{Im}), 123.8 (CH_{Im}), 119.9 (C_{Ar}), 117.0 (CN), 112.3 (CH_{Ar}), 103.4 (C_{Ar}), 82.0 ($O\underline{C}(CH_3)_3$), 80.4 ($O\underline{C}(CH_3)_3$), 70.6 (OCH_2), 48.5 ($\underline{C}H_2CH_2NHCON$), 47.5 ($OCH_2\underline{C}H_2$), 44.3 ($ImCH_2N$), 44.0 ($\underline{C}H_2CH_2NHBoc$), 39.8 ($CH_2\underline{C}H_2NHCON$), 39.5 ($CH_2\underline{C}H_2NHBoc$), 29.2 ($CH_3$), 29.0 ($CH_3$); HRMS (ESI positive, *m/z*): calculated for $C_{28}H_{39}N_7O_6$ 569.2962; found 569.2976 (2.56 ppm)

tert-Butyl (2-((tert-butoxycarbonyl)amino)ethyl)((1-(4-carbamothioyl-3-(2-(2-oxoimidazolidin-1-yl)ethoxy)phenyl)-1H-imidazol-2-yl)methyl)carbamate **(27)**. A solution of the nitrile **26** (64 mg, 0.112 mmol) in dry DMF (5 mL) was treated with 20% $(NH_4)_2S$ (aq) (0.66 ml, 1.941 mmol) . The reaction mixture was stirred at 80 °C for 3 h. Then, water was added (50 mL) and the reaction was extracted with DCM (3 x 40 mL). The organic layer was dried (Na_2SO_4), filtered and concentrated

to dryness under reduced pressure. The orange residue was purified by flash column chromatography (DCM/MeOH, 9.75 : 0.25) to give 70 mg (98% yield) of the thioamide **27** as a yellow oil. ^{1}H NMR (CD_3OD, 400 MHz) δ (ppm): 8.30 - 8.21 (m, 2H, Ar), 8.05 (bs, 1H, $SCNH_2$), 7.98 (bs, 1H, $SCNH_2$) 7.29 (d, J = 1.4 Hz, 1H, Ar), 7.06 (s, 1H, Ar), 7.02 (dd, J = 8.3, 1.9 Hz, 1H, Ar), 4.72 - 4.52 (m, 2H, ImCH_2N), 4.36 - 4.20 (m, 2H, OCH_2CH_2), 3.81 - 3.51 (m, 4H, CH_2CH_2NHCON, OCH_2CH_2), 3.41 (dd, J = 9.2, 6.9 Hz, 2H, CH_2CH_2NHCON), 3.23 - 3.06 (m, 4H, CH_2CH_2NHBoc), 1.40 (s, 9H, CH_3), 1.35 (s, 9H, CH_3); ^{13}C NMR (CD_3OD, 125 MHz) δ (ppm): 210.0 ($SCNH_2$), 166.0 (C_{Ar}), 165.1 (C_{Ar}), 164.8 (C_{Ar}), 156.6 (NHCOO), 156.3 (NHCOO), 145.8 (C_{Ar}), 141.3 (C_{Ar}), 135.7 (CH_{Ar}), 128.4 (CH_{Ar}), 123.4 (CH_{Im}), 123.4 (CH_{Im}), 118.4 (CH_{Ar}), 111.4 (C_{Ar}), 81.6 (O$C(CH_3)_3$), 80.8 (O$C(CH_3)_3$), 68.6 (OCH_2), 49.8 (CH_2CH_2NHCON), 46.9 (OCH_2CH_2), 44.0 ($ImCH_2N$), 39.3 (CH_2CH_2NHBoc), 36.9 (CH_2CH_2NHCON), 30.7 (CH_2CH_2NHBoc), 28.8 (CH_3), 28.6 (CH_3); HRMS (ESI positive, *m/z*): calculated for $C_{28}H_{41}N_7O_6S$ 603.2839; found 603.2830 (-1.43 ppm)

General procedure for the Hantzsch thiazole synthesis of 36a-f. The intermediate thioamide **27** (1 equiv) and the appropriated commercially available α-haloketones or synthetic analogues **32-35** (1.1 equiv) in isopropanol (25 mL) was added to a pressure flask. The pressure flask was stirred at 70 °C for 4 h and the solvent was eliminated to dryness. The residue was purified by flash column chromatography (DCM/MeOH, 9 : 1) to give the thiazoles **36a-f** as a colourless oil.

General procedure for hydrogenation of the double bond of 36e,f. A solution of the unsaturated analogues **36e,f** (1 equiv) in THF/MeOH, 1:1 (30 mL) containing Pd/C (10%) (20% wt/wt) was hydrogenated at room temperature for 2 h under atmospheric pressure using a balloon filled with hydrogen gas (3 cycles of vacuum + hydrogen). The Pd/C was filtered through Whatman PTFE filter paper and the solvent was removed under reduced pressure. The residue was purified by CCTLC on the Chromatotron (DCM/MeOH, 9.5:0.5) to afford **37e,f** as a colourless oil.

General procedure for deprotection of the Boc group. The protected di-Boc derivatives **36a-d** and **37e,f** (1 equiv) were dissolved in DCM (20 mL) and were reacted with TFA (1 mL) at room temperature for 2 h. The excess of TFA was removed under reduced pressure coevaporating several times with DCM and MeOH to give the final deprotected analogues **3a-f** as a colourless oil quantitatively.

N^1-((1-(4-(4-Isobutylthiazol-2-yl)-3-(2-(2-oxoimidazolidin-1-yl)ethoxy)phenyl)-1H-imidazol-2-yl)methyl)ethane-1,2-diaminium 2,2,2-trifluoroacetate **(3a)**. ^{1}H NMR (CD_3OD, 400 MHz) δ (ppm): 8.52 (d, *J* = 8.4 Hz, 1H, Ar), 7.78 (d, *J* = 2.0 Hz, 1H, Ar), 7.64 (d, *J* = 2.0 Hz, 1H, Ar), 7.48 (d, *J* = 2.0 Hz, 1H, Ar), 7.33 - 7.26 (m, 2H, Ar), 4.49 (t, *J* = 5.6 Hz, 2H, $OC\underline{H_2}CH_2$), 4.22 (s, 2H, $ImC\underline{H_2}NH$), 3.73 (t, *J* = 5.5 Hz, 2H, $OCH_2C\underline{H_2}$), 3.63 (dd, *J* = 9.3, 6.9 Hz, 2H, $C\underline{H_2}CH_2NHCON$), 3.38 (dd, *J* = 9.2, 6.9 Hz, 2H, $CH_2C\underline{H_2}NHCON$), 3.08 (dd, *J* = 6.8, 4.9 Hz, 2H, $C\underline{H_2}CH_2NH_3^+$), 3.00 (dd, *J* = 6.7, 4.8 Hz, 2H, $CH_2C\underline{H_2}NH_3^+$), 2.72 (d, *J* = 7.1 Hz, 2H, $C\underline{H_2}CH(CH_3)_2$), 2.20 - 2.06 (m, 1H, $CH_2C\underline{H}(CH_3)_2$), 0.98 (d, *J* = 6.7 Hz, 6H, $CH_2CH(C\underline{H_3})_2$); ^{13}C NMR ($CD_3OD$, 75 MHz) δ (ppm): 165.1 (NHCON), 161.2 (OC_{Ar}), 157.4 (C_{Ar}), 157.2 (C_{Ar}), 147.3 (C_{Ar}), 137.2 (C_{Ar}), 130.9 (CH_{Ar}), 125.6 (CH_{Im}), 124.8 (CH_{Im}), 121.9 (CH_{Ar}), 119.3 (CH_{Ar}), 117.9 (CH_{Ar}), 111.7 (C_{Ar}), 68.2 (OCH_2), 46.9 ($ImCH_2$), 46.8 ($\underline{C}H_2CH_2NHCON$), 44.3 ($\underline{C}H_2CH_2NH_3^+$), 43.5 ($OCH_2\underline{C}H_2$), 41.4 ($ThiazCH_2$), 39.6 ($CH_2NH_3^+$), 39.3 ($CH_2\underline{C}H_2NHCON$), 29.9 ($\underline{C}H(CH_3)_3$), 22.7 ($CH_3$); HPLC (10% to 100% of acetonitrile in 15 min), Rt = 3.4 min; HRMS (ESI positive, *m/z*): calculated for $C_{24}H_{33}N_7O_2S$ 483.2416; found 483.2412 (-0.86 ppm); Anal. Calcd. for $C_{30}H_{35}F_9N_7O_8S$: C. 43.64; H. 4.39; N. 11.87; S. 3.88; Found: C. 44.15; H. 4.83; N. 11.97; S. 3.90

N^1-((1-(4-(4-Neopentylthiazol-2-yl)-3-(2-(2-oxoimidazolidin-1-yl)ethoxy)phenyl)-1H-imidazol-2-yl)methyl)ethane-1,2-diaminium 2,2,2-trifluoroacetate **(3b)**. ^{1}H NMR (CD_3OD, 400 MHz) δ (ppm): 8.53 (d, *J* = 8.4 Hz, 1H, Ar), 7.78 (d, *J* = 2.0 Hz, 1H, Ar), 7.64 (d, *J* = 2.0 Hz, 1H, Ar), 7.48 (d, *J* = 2.1 Hz, 1H, Ar), 7.34 - 7.26 (m, 2H, Ar), 4.49 (t, *J* = 5.6 Hz, 2H, $OC\underline{H_2}CH_2$), 4.24 (s, 2H, $ImC\underline{H_2}NH$), 3.73 (t, *J* = 5.5 Hz, 2H, $OCH_2C\underline{H_2}$), 3.63 (dd, *J* = 9.3, 6.9 Hz, 2H, $C\underline{H_2}CH_2NHCON$),

3.38 (dd, *J* = 9.2, 6.9 Hz, 2H, $CH_2C\underline{H_2}NHCON$), 3.10 (dd, *J* = 6.5, 4.5 Hz, 2H, $C\underline{H_2}CH_2NH_3^+$), 3.03 (dd, *J* = 6.6, 4.6 Hz, 2H, $CH_2C\underline{H_2}NH_3^+$), 2.77 (s, 2H, $C\underline{H_2}C(CH_3)_3$), 1.00 (s, 9H, CH_3); ^{13}C NMR (CD_3OD, 75 MHz) δ (ppm): 165.1 (NHCON), 160.4 (OC_{Ar}), 157.2 (C_{Ar}), 156.1 (C_{Ar}), 147.2 (C_{Ar}), 137.1 (C_{Ar}), 130.9 (CH_{Ar}), 125.7 (CH_{Im}), 124.8 (CH_{Im}), 121.9 (CH_{Ar}), 119.3 (CH_{Ar}), 119.1 (CH_{Ar}), 111.7 (C_{Ar}), 68.2 (OCH_2), 46.8 ($\underline{C}H_2CH_2NHCON$), 45.7 ($ThiazCH_2$), 44.3 ($\underline{C}H_2CH_2NH_3^+$), 43.5, ($OCH_2\underline{C}H_2$) 39.6 ($CH_2NH_3^+$), 39.3 ($CH_2\underline{C}H_2NHCON$), 32.4 ($\underline{C}(CH_3)_3$), 30.0 ($CH_3$); HPLC (10% to 100% of acetonitrile in 15 min), Rt = 3.4 min; HRMS (ESI positive, *m/z*): calculated for $C_{25}H_{35}N_7O_2S$ 497.2573; found 497.2562 (-2.19 ppm); Anal. Calcd. for $C_{31}H_{38}F_9N_7O_8S$: C. 44.34; H. 4.56; N. 11.68; S. 3.82; Found: C. 44.05; H. 4.68; N. 11.77; S. 3.52

N^1*-((1-(4-(4-Benzylthiazol-2-yl)-3-(2-(2-oxoimidazolidin-1-yl)ethoxy)phenyl)-1H-imidazol-2-yl)methyl)ethane-1,2-diaminium 2,2,2-trifluoroacetate* (**3c**). ^{1}H NMR (CD_3OD, 400 MHz) δ (ppm): 8.51 (d, *J* = 8.4 Hz, 1H, Ar), 7.77 (d, *J* = 1.9 Hz, 1H, Ar), 7.64 (d, *J* = 1.9 Hz, 1H, Ar), 7.48 (d, *J* = 2.0 Hz, 1H, Ar), 7.40 - 7.25 (m, 5H, Ar), 7.24 - 7.18 (m, 2H, Ar), 4.47 (t, *J* = 5.5 Hz, 2H, $OC\underline{H_2}CH_2$), 4.26 (s, 2H, $ImC\underline{H_2}NH$), 4.19 (s, 2H, CH_2Ph), 3.71 (t, *J* = 5.5 Hz, 2H, $OCH_2C\underline{H_2}$), 3.59 (dd, *J* = 9.3, 6.9 Hz, 2H, $C\underline{H_2}CH_2NHCON$), 3.35 (dd, *J* = 9.3, 6.9 Hz, 2H, $CH_2C\underline{H_2}NHCON$), 3.11 (dd, *J* = 6.2, 4.5 Hz, 2H, $C\underline{H_2}CH_2NH_3^+$), 3.06 (dd, *J* = 4.5, 2.8 Hz, 2H, $CH_2C\underline{H_2}NH_3^+$); ^{13}C NMR ($CD_3OD$, 75 MHz) δ (ppm): 165.1 (NHCON), 160.4 (OC_{Ar}), 157.3 (C_{Ar}), 157.2 (C_{Ar}), 146.9 (C_{Ar}), 140.7 (C_{Ar}), 137.3 (C_{Ar}), 130.9 (CH_{Ar}), 130.0 (CH_{Ar}), 129.5 (CH_{Ar}), 127.4 (CH_{Ar}), 125.4 (CH_{Im}), 124.8 (CH_{Im}), 122.0 (CH_{Ar}), 119.3 (CH_{Ar}), 118.3 (CH_{Ar}), 114.1 (C_{Ar}), 111.7 (C_{Ar}), 68.1 (OCH_2), 46.8 ($ImCH_2$), 46.7 ($\underline{C}H_2CH_2NHCON$), 44.2 ($\underline{C}H_2CH_2NH_3^+$), 43.4 ($OCH_2\underline{C}H_2$), 39.5 ($CH_2NH_3^+$), 39.3 ($CH_2\underline{C}H_2NHCON$), 38.4 ($ThiazCH_2$); HPLC (10% to 100% of acetonitrile in 15 min), Rt = 3.8 min; HRMS (ESI positive, *m/z*): calculated for $C_{27}H_{31}N_7O_2S$ 517.2560; found 517.2560 (-0.09 ppm); Anal. Calcd. for $C_{33}H_{34}F_9N_7O_8S$: C. 46.10; H. 3.99; N. 11.40; S. 3.73; Found: C. 45.75; H. 4.46; N. 11.64; S. 3.70

N^{1}*-((1-(3-(2-(2-Oxoimidazolidin-1-yl)ethoxy)-4-(4-phenethylthiazol-2-yl)phenyl)-1H-imidazol-2-yl)methyl)ethane-1,2-diaminium 2,2,2-trifluoroacetate* **(3d)**. ^{1}H NMR (CD_3OD, 400 MHz) δ (ppm): 8.55 (d, *J* = 8.4 Hz, 1H, Ar), 7.79 (d, *J* = 2.0 Hz, 1H, Ar), 7.65 (d, *J* = 2.0 Hz, 1H, Ar), 7.49 (d, *J* = 2.1 Hz, 1H, Ar), 7.31 (dd, *J* = 8.4, 2.0 Hz, 1H, Ar), 7.28 - 7.04 (m, 6H, Ar), 4.49 (t, *J* = 5.6 Hz, 2H, $OC\underline{H_2}CH_2$), 4.23 (s, 2H, $ImC\underline{H_2}NH$), 3.75 (t, *J* = 5.5 Hz, 2H, $OCH_2C\underline{H_2}$), 3.62 (dd, *J* = 9.1, 7.1 Hz, 2H, $C\underline{H_2}CH_2NHCON$), 3.37 (dd, *J* = 9.3, 6.9 Hz, 2H, $CH_2C\underline{H_2}NHCON$), 3.19 - 3.13 (m, 2H), 3.11 - 3.05 (m, 4H), 3.04 - 2.95 (m, 2H); ^{13}C NMR (CD_3OD, 75 MHz) δ (ppm): 165.1 (NHCON), 161.4 (OC_{Ar}), 157.3 (C_{Ar}), 157.2 (C_{Ar}), 147.2 (C_{Ar}), 142.7 (C_{Ar}), 137.2 (C_{Ar}), 130.9 (CH_{Ar}), 129.5 (CH_{Ar}), 129.4 (CH_{Ar}), 127.0 (CH_{Ar}), 125.5 (CH_{Im}), 124.9 (CH_{Im}), 121.9 (CH_{Ar}), 119.3 (CH_{Ar}), 117.6 (CH_{Ar}), 111.7 (C_{Ar}), 68.2 (OCH_2), 46.8 ($\underline{C}H_2CH_2NHCON$), 44.3 ($\underline{C}H_2CH_2NH_3^+$), 43.5 ($OCH_2\underline{C}H_2$), 39.6 ($CH_2NH_3^+$), 39.3 ($CH_2\underline{C}H_2NHCON$), 36.6 ($ThiazCH_2CH_2$), 34.3 ($ThiazCH_2CH_2$); HPLC (10% to 100% of acetonitrile in 15 min), Rt = 3.6 min; HRMS (ESI positive, *m/z*): calculated for $C_{28}H_{33}N_7O_2S$ 531.2416; found531.2424 (1.52 ppm); Anal. Calcd. for $C_{34}H_{36}F_9N_7O_8S$: C. 46.74; H. 4.15; N. 11.22; S. 3.67; Found: C. 47.01; H. 4.43; N. 11.36; S. 3.31

N^{1}*-((1-(4-(4-(2-(Naphthalen-2-yl)ethyl)thiazol-2-yl)-3-(2-(2-oxoimidazolidin-1-yl)ethoxy)phenyl)-1H-imidazol-2-yl)methyl)ethane-1,2-diaminium 2,2,2-trifluoroacetate* **(3e)**. ^{1}H NMR (CD_3OD, 400 MHz) δ (ppm): 8.54 (d, *J* = 8.4 Hz, 1H, Ar), 7.89 - 7.70 (m, 4H, Ar), 7.64 (d, *J* = 1.9 Hz, 1H, Ar), 7.48 (d, *J* = 2.0 Hz, 1H, Ar), 7.45 - 7.33 (m, 3H), 7.30 (dd, *J* = 8.4, 2.0 Hz, 1H, Ar), 7.23 (s, 1H, Ar), 4.48 (t, *J* = 5.6 Hz, 2H, $OC\underline{H_2}CH_2$), 4.23 (s, 2H, $ImC\underline{H_2}NH$), 3.71 (t, *J* = 5.5 Hz, 2H, $OCH_2C\underline{H_2}$), 3.59 (dd, *J* = 9.3, 6.9 Hz, 2H, $C\underline{H_2}CH_2NHCON$), 3.26 (s, 4H), 3.09 (dd, *J* = 6.5, 4.6 Hz, 2H, $C\underline{H_2}CH_2NH_3^+$), 3.02 (dd, *J* = 7.2, 5.2 Hz, 2H, $CH_2C\underline{H_2}NH_3^+$); ^{13}C NMR ($CD_3OD$, 75 MHz) δ (ppm): 165.0 (NHCON), 162.8 (OC_{Ar}), 157.2 (C_{Ar}), 157.2 (C_{Ar}), 147.2 (C_{Ar}), 140.2 (C_{Ar}), 137.2 (C_{Ar}), 135.1 (C_{Ar}), 133.6 (CH_{Ar}), 130.9 (CH_{Ar}), 128.9 (CH_{Ar}), 128.6 (CH_{Ar}), 128.4 (CH_{Ar}), 128.3 (CH_{Ar}), 127.6 (C_{Ar}), 126.9 (CH_{Ar}), 126.2 (CH_{Ar}), 125.5 (CH_{Im}), 124.8 (CH_{Im}), 122.0 (CH_{Ar}), 119.3 (CH_{Ar}), 117.7 (CH_{Ar}), 111.7 (C_{Ar}), 68.2 (OCH_2), 49.9 ($ImCH_2$), 46.8 ($\underline{C}H_2CH_2NHCON$), 44.3

($\underline{C}H_2CH_2NH_3^+$), 43.5 ($OCH_2\underline{C}H_2$), 39.6 ($CH_2NH_3^+$), 39.2 ($CH_2\underline{C}H_2NHCON$), 36.8 ($ThiazCH_2CH_2$), 34.0 ($ThiazCH_2CH_2$); HPLC (10% to 100% of acetonitrile in 15 min), Rt = 6.7 min; HRMS (ESI positive, *m/z*): calculated for $C_{32}H_{35}N_7O_2S$ 581.2573; found 581.2563 (-1.67 ppm); Anal. Calcd. for $C_{38}H_{38}F_9N_7O_8S$: C. 49.41; H. 4.15; N. 10.61; S. 3.47; Found: C. 48.95; H. 4.62; N. 10.37; S. 4.21

N^1-((1-(4-(4-(2-([1,1'-Biphenyl]-4-yl)ethyl)thiazol-2-yl)-3-(2-(2-oxoimidazolidin-1-yl)ethoxy)phenyl)-1H-imidazol-2-yl)methyl)ethane-1,2-diaminium 2,2,2-trifluoroacetate **(3f)**. ^1H NMR (CD_3OD, 400 MHz) δ (ppm): 8.55 (d, *J* = 8.4 Hz, 1H, Ar), 7.78 (d, *J* = 2.0 Hz, 1H, Ar), 7.65 (d, *J* = 1.9 Hz, 1H, Ar), 7.60 - 7.56 (m, 2H, Ar), 7.54 - 7.49 (m, 2H, Ar), 7.48 (d, *J* = 2.0 Hz, 1H, Ar), 7.41 (t, *J* = 7.6 Hz, 2H, Ar), 7.35 - 7.25 (m, 5H), 4.49 (t, *J* = 5.6 Hz, 2H, $OC\underline{H_2}CH_2$), 4.24 (s, 2H, $ImC\underline{H_2}NH$), 3.72 (t, *J* = 5.5 Hz, 2H, $OCH_2C\underline{H_2}$), 3.61 (dd, *J* = 9.1, 7.1 Hz, 2H, $C\underline{H_2}CH_2NHCON$), 3.35 (dd, *J* = 9.1, 7.1 Hz, 2H, $NHCONCH_2C\underline{H_2}$), 3.24 - 3.12 (m, 4H, $C\underline{H_2}C\underline{H_2}BiPh$) 3.10 (dd, *J* = 6.6, 4.7 Hz, 2H, $C\underline{H_2}CH_2NH_3^+$), 3.03 (dd, *J* = 7.0, 5.0 Hz, 2H, $CH_2C\underline{H_2}NH_3^+$); ^{13}C NMR (CD_3OD, 100 MHz) δ (ppm): 165.1 (NHCON), 162.0 (OC_{Ar}), 161.4 (C_{Ar}), 157.3 (C_{Ar}), 147.1 (C_{Ar}), 142.3 (C_{Ar}), 141.9 (C_{Ar}), 140.2 (C_{Ar}), 137.2 (C_{Ar}), 130.9 (CH_{Ar}), 130.0 (CH_{Ar}), 129.8 (CH_{Ar}), 128.1 (CH_{Ar}), 127.9 (CH_{Ar}), 127.8 (CH_{Ar}), 125.6 (CH_{Im}), 124.9 (CH_{Im}), 121.9 (CH_{Ar}), 119.3 (CH_{Ar}), 117.7 (C_{Ar}), 111.7 (C_{Ar}), 68.2 (OCH_2), 46.8 ($\underline{C}H_2CH_2NHCON$), 44.2 ($\underline{C}H_2CH_2NH_3^+$), 43.5 ($OCH_2\underline{C}H_2$), 39.6 ($CH_2NH_3^+$), 39.3 ($CH_2\underline{C}H_2NHCON$), 36.2 ($ThiazCH_2CH_2$), 34.1 ($ThiazCH_2CH_2$); HPLC (10% to 100% of acetonitrile in 15 min), Rt = 7.5 min; HRMS (ESI positive, *m/z*): calculated for $C_{34}H_{37}N_7O_2S$ 607.2729; found 607.2739 (1.57 ppm); Anal. Calcd. for $C_{40}H_{40}F_9N_7O_8S$: C. 50.58; H. 4.24; N. 10.32; S. 3.38; Found: C. 50.15; H. 4.38; N. 9.83; S. 3.20

Experimental water-solubility studies. Water-solubility of proteomimetics **3a-f** was determined by HPLC analysis. The HPLC runs were carried out on a Waters 484 System using Novapack C18 reverse phase column. Flow rate: 1 mL/min. Detection: UV 254 nm. Gradient solvent system A/B (acetonitrile/water): initial 10% A + 90% B; 10 min linear gradient to 100% B; Excess amount of the compounds was suspended in deionized water (pH = 5.5), sonicated for 10

min at room temperature, and then equilibrated overnight at room temperature. The samples were centrifuged at 14,000 rpm in an eppendorf microcentrifuge for 1.5 min at room temperature. An aliquot of the clear supernatant was removed and diluted to a concentration within the range of a five-point standard curve. Water solubility was calculated by HPLC analysis by comparing the peak areas of each compound with those of standard solutions of the compounds in DMSO with a known concentration.

Biological methods. *Li*-TryR oxidoreductase activity. Oxidoreductase activity was determined according to the method described by Hamilton et al.[41] Briefly, reactions were carried out at 26 ºC (250 µl) of HEPES pH 8.0 (40 mM) buffer containing EDTA (1 mM), NADPH (150 µM), NADP+ (30 µM), DTNB (25 µM), T[S]2 (1 µM), glicerol (0.02%), DMSO (1.5%) and recombinant *Li*-TryR (7 nM). For IC_{50} determinations (**2a-i** and **3a-f**) the enzyme was pre-incubated with the compounds (concentrations ranging from 75 µM to 0.29 µM) for 10 min prior to the addition of $T[S]_2$ and NADPH. Enzyme activity was monitored by the increase in absorbance at 412 nm for 1 h at 26 °C in an EnSpire Multimode Plate Reader (PerkinElmer, Waltham, MA, USA). All the assays were conducted in triplicate in at least three independent experiments. Data were analyzed using a nonlineal regression model with the Grafit6 software (Erithacus, Horley, Surrey, UK).

Dimer quantitation assay. The stability of the *Li*-TryR dimeric form in the presence of compounds **2a-i** and **3a-f** was evaluated using the novel Enzyme-Linked ImmunoSorbent Assay (ELISA) recently developed in our laboratory.[14] Briefly a dual (HIS/FLAG) tagged *Li*-TryR (400 nM) was incubated in a dimerization buffer (1mL 300 mM NaCl, 50 mM Tris pH 8.0) for 16 h at 37 °C with agitation and in a humid atmosphere in the presence of the different compounds (20 μM). Next the different solutions were centrifuged at 18000xg for 15 minutes at room temperature. The supernatatnts (200 μL/well) were added to the α-FLAG (Sigma–Aldrich, St. Louis, MO, USA) coated plates and incubated for 30 minutes at 37 °C with agitation in a humid atmosphere. The plates were washed five times with TTBS (0.1% Tween, 2 mM Tris, 138 mM NaCl 138 pH 7.6)

and incubated with diluted monoclonal α-HIS HRP conjugated antibody (200 µl, 1:50000, Abcam, Cambridge, UK) in BSA (5%) in TTBS for 1 h at room temperature. The plates were washed once again as previously described and *o*-phenylenediamine dihydrochloride (OPD) substrate (Sigma–Aldrich, St. Louis, MO, USA) prepared according to manufacturer's instructions was added. The enzymatic reaction was stopped after 10 min with H_2SO_4 (100 µL, 0.5 M) and the absorbances were measured at 490 nm in an EnSpire Multimode Plate Reader (PerkinElmer, Waltham, MA, USA). All the assays were conducted in triplicate in at least three independent experiments. Data were analyzed using a non-linear regression model with the GraFit 6 software (Erithacus, Horley, Surrey, UK).

Cells and culture conditions. *L. infantum* axenic amastigotes (MCAN/ES/ 89/IPZ229/1/89) were grown in M199 (Invitrogen, Leiden, The Netherlands) medium supplemented with 10% heat inactivated FCS, 1 g/L β-alanine, 100 mg/L L-asparagine, 200 mg/L sucrose, 50 mg/L sodium pyruvate, 320 mg/L malic acid, 40 mg/L fumaric acid, 70 mg/L succinic acid, 200 mg/L α-ketoglutaric acid, 300 mg/L citric acid, 1.1 g/L sodium bicarbonate, 5 g/L MES, 0.4 mg/L hemin, 10 mg/L gentamicine pH 5.4 at 37 ºC. THP-1 cells were grown in RPMI-1640 medium (Gibco, Leiden, The Netherlands) supplemented with 10% heat inactivated FCS, antibiotics, 1 mM HEPES, 2 mM glutamine and 1 mM sodium pyruvate, pH 7.2 at 37 ºC and 5% CO_2.

L. infantum promastigotes (MCAN/ES/ 89/IPZ229/1/89) were grown in RPMI-1640 medium (Sigma–Aldrich, St. Louis, MO, USA) supplemented with 10% heat-inactivated fetal calf serum (FCS), antibiotics, and 25 mm HEPES (pH 7.2) at 26 ºC.

Leishmanicidal activity. Drug treatment of amastigotes was performed during the logarithmic growth phase at a concentration of 1×10^6 parasites/mL at 37 ºC for 24 h. Drug treatment of promastigotes was performed during the logarithmic growth phase at a concentration of 2×10^6 parasites/mL at 26 ºC for 24 h. EC_{50} was evaluated by flow cytometry by the propidium iodide (PI) exclusion method.[47] After selection of the parasite population based on their forward scatter (FSC)

and side scatter (SSC) values, live and dead parasite cells were identified by their permeability to PI. To minimize the presence of fragmented parasites drug treatment never exceeded 24 h. Data were analyzed using a non-linear regression model with the GraFit 6 software (Erithacus, Horley, Surrey, UK).

Cytotoxicity assays. Drug treatment of THP-1 monocyte-derived macrophages was performed at a concentration of 10^6 cells/mL at 37 ºC and 5% CO_2 for 24 h. EC_{50} was evaluated by the crystal violet assay. Briefly, cells were washed with PBS and stained with 200 µl of crystal violet (0.2% crystal violet, 2% ethanol) during 10 minutes at room temperature. Next the plates were washed twice in tap water by immersion in two large trays and allowed to dry. The stained cells were solubilized with 400 µL of 1% SDS and color intensity was quantified at 570 nm using an EnSpire Multimode Plate Reader (PerkinElmer, Waltham, MA, USA). All the assays were conducted in triplicate in at least three independent experiments. Data were analyzed using a non-linear regression model with the GraFit 6 software (Erithacus, Horley, Surrey, UK).

Fluorescence microscopy. Logarithmic growth phase promastigotes were treated with 25 μM of either **3e** or **3f** for 1 h at 26 ºC. Parasites were fixed using a solution containing EDTA (450 mM) and mounted on polysine slides (Thermo Scientific, Waltham, MA, USA). Images were captured with an Eclipse Ti inverted microscope (Nikon, Tokyo, Japan).

Crystal structure determination of *Li*-TryR:2f complex. *Li*-TryR sample used for crystallization was at 7.5 mg/mL in 20 mM Tris buffer pH 8. Native protein crystals were obtained by the hanging drop vapour diffusion method, mixing 1 µl protein sample with 1 µl well solution (0.1 M Tris-HCl pH 8, 2.2 M $(NH_4)_2SO_4$, 500 µl reservoir volume). Yellow bi-pyramidal crystals grew up in two days and were then used for soaking experiments.

Li-TryR crystals were soaked in a solution with **2f** ligand (0.1 M Tris-HCl pH 8, 2.2 M $(NH_4)_2SO_4$, 25 mM **2f**) for 16 h and then cryoprotected in a modified reservoir solution containing 25% glycerol.

Single wavelength (λ=0.979 Å) diffraction data was collected at beamline BL-13 (XALOC) of the ALBA Synchrotron (Barcelona, Spain) at 100K. XDS[48] program was used for indexing images and integration and AIMLESS from CCP4[49] software package for scaling and merging the data. 5 % of the diffraction data were reserved for cross-validation. The structure was solved by the molecular replacement method with MOLREP[50] using *Li*-TryR (PDB ID: 2JK6) as the search model. Two monomers were found in the asymmetric unit that were then refined using REFMAC,[51] employing tight geometric and noncrystallographic symmetry restraints, jelly-body refinement and map sharpening. Model building was carried out using the program COOT.[52] Crystal parameters, data collection and relevant statistics are listed in Table S2 in Supplementary Information.

Computational methods. The ground state geometry of **3f** was optimized in the gas phase and its electrostatic potential was computed at the HF/6-31G**//HF/3-21G level of theory. AMBER atom types were assigned from the *leaprcff14SB* force field and atom-centered RESP charges were calculated using the antechamber module in AmberTools18 (http://ambermd.org). **3f** was manually superimposed at the dimer interface of *Li*-TryR, as found in PDB entry 2JK6.[53] The amidinium, amide and biphenyl groups of **3f** were oriented in the same way as the side chains of residues Glu436', Gln440' and Ile442 located in the Pro435-Met447α-helix. The *Li*-TryR:**3f** and *Li*-TryR:**1a** complexes were simulated as reported previously[14,16] by using the GPU-based implementation of the *pmemd.cuda* module of Amber16 in the Single-Precision-Fixed-Precision (SPFP) mode. The force field parameters for the FAD cofactor were taken from the Bryce's group site (http://research.bmh.manchester.ac.uk/bryce/amber/). Briefly, each complex was immersed in a box of ca. 27000 TIP3P water molecules that extended 12 Å away from any solute atom and 5 Na^+ ions were added to ensure charge neutrality. The Cα positions of the *Li*-TryR monomer were positionally restrained with a harmonic restraint of 1 kcal mol^{-1} $Å^{-2}$ for the first 10 ns (300 K, time step of 2 fs) to preserve the secondary structure but were removed for the remaining 20 ns. The cutoff distance for the nonbonded interactions was 10 Å and periodic boundary conditions were

used. Electrostatic interactions were treated by means of the smooth particle mesh Ewald (PME) method with a grid spacing of 1 Å and the SHAKE algorithm was applied to all bonds involving hydrogen atoms. The binding energy analysis was carried out with our in-house tool MM-ISMSA.[54] 20 snapshots of the last 90 ns of the MD simulations were cooled-down from 300 to 100 K during 1 ns. The final geometries were used for the energy analysis. The MD trajectories were analyzed using the *cpptraj* module of AmberTools18. The 3D pharmacophore model for the pyrrolopyrimidine series **2a-2i** was generated using the LigandScout software.[55]

ASSOCIATED CONTENT

Supporting information

The supporting information is available free of charge on the ACS publications website at DOI:

Details of: (i) chemical synthesis of intermediates **12a-g**, **18-20**, **24,** α-bromo ketone intermediates **32-35, 36a-f, 37e-f** and compounds characterization, (ii) physicochemical parameters of compounds **3a-f** and fluorescence spectra of compound **3d**, (iii) further X-ray crystallography data, (iv) further computational studies and v) ^{1}H and ^{13}C NMR spectra of selected compounds.

AUTHOR INFORMATION

Corresponding Author

* Tel. 34-912587689. E-mail: sonsoles@iqm.csic.es

ORCID

Alejandro Revuelto: 0000-0002-0226-040X

Marta Ruiz-Santaquiteria: 0000-0001-7942-5949

Héctor de Lucio: 0000-0002-9840-0779

Alejandra Angela Carriles: 0000-0003-0481-2551

Pedro A. Sánchez-Murcia: 0000-0001-8415-870X

Juan Hermoso: 0000-0002-1863-8950

Federico Gago: 0000-0002-3071-4878

Antonio Jiménez-Ruiz: 0000-0001-8238-3081

María-José Camarasa: 0000-0002-4978-6468

Sonsoles Velázquez: 0000-0003-2209-1751

Author contributions

The manuscript was written through contributions of all authors. All authors have given approval to the final version of the manuscript.

Notes

The authors declare no competing financial interest

ACKNOWLEDGEMENTS

We thank the Spanish Government (MINECO/FEDER Projects SAF2015-64629-C2, BFU2017-90030-P), the Comunidad de Madrid (BIPEDD-2-CM ref. S-2010/BMD-2457) and the Consejo Superior de Investigaciones Científicas (CSIC Project 201980E028) for financial support. We thank staff from ALBA Synchrotron (Barcelona, Spain) for support during data collection.

ABBREVIATIONS

ELISA, Enzyme-Linked ImmunoSorbent Assay; IC_{50}, inhibitory concentration 50; EC_{50}, effective concentration 50; GR, glutathione reductase; *Li*-TryR, *Leishmania infantum* trypanothione reductase; NTDs, neglected tropical diseases; PPIs, protein-protein interaction inhibitors; PI, propidium iodide; SN_Ar, nucleophilic aromatic substitution; Try/TryR, thypanothione/trypanothione reductase; VL, visceral leishmaniasis

REFERENCES

(1) http://www.who.int/leishmaniasis/en/ updated March 2018

(2) Zulfigar, B., Shelper, T. B., Avery, V. M. (2017) Leishmaniasis drug discovery: recent progress and challenges in assay development, *Drug discovery today*, 22, 1516-1531 DOI 10.1016/j.drudis.2017.06.004.

(3) Field, M. C., Horn, D., Fairlamb, A. H., Ferguson, M. A. J., Gray, D. W., Read, K. D., Rycker, M. D., Torrie, L. S., Wyatt, P. G., Wyllie, S., Gilbert, I. A. (2017) Anti-trypanosomatid drug discovery: an ongoing challenge and a continuing need, *Nat. Rev. Microbiol.* 15, 217-231 DOI 10.1038/nrmicro.2016.193.

(4) Sangshetti, J. N., Khan, F. A. K., Kulkarni, A. A., Arote R., Patil R. H. (2015) Antileishmanial drug discovery: comprehensive review of the last 10 years. *RSC Adv.*, 5, 32376-32415 DOI 10.1039/C5RA02669E.

(5) Nagle, A. S., Khare, S., Kumar, A. B., Supek, F., Buchynskyy, A., Mathison, C. J. N., Chennamaneni, N. K., Pendem, N., Buckner, F. S., Gelb, M. H., Molteni, V. (2014) Recent developments in drug discovery for leishmaniasis and human african trypanosomiasis, *Chem. Rev.* 114, 11305-11347 DOI 10.1021/cr500365f.

(6) Alcolea, P. J., Alonso, A., Larraga, V. (2016) Rationale for selection of developmentally regulated genes as vaccine candidates against *Leishmania infantum* infection, *Vaccine*. 34, 5474-5478 DOI 10.1016/j.vaccine.2016.08.081.

(7) Frearson, J. A., Wyatt, P. A., Gilbert, I. H., Fairlamb, A. H. (2007) Target assessment for antiparasitic drug discovery. *Trends Parasitol*. 23, 589-595 DOI 10.1016/j.pt.2007.08.019.

(8) Krauth-Siegel, R. L., Meiering, S. K., Schmidt, H. (2003) The parasite-specific trypanothione metabolism of trypanosoma and leishmania, *Biol. Chem*. 384, 539-549 DOI 10.1515/BC.2003.062.

(9) Leroux, E. A., Krauth-Siegel, R. L. (2016) Thiol redox biology of trypanosomatids and potential targets for chemotherapy, *Mol. Biochem. Parasitol.* 206, 67-74 DOI 10.1016/j.molbiopara.2015.11.003.

(10) Vijayakumar, S., Das, P. (2018) Recent progress in drug targets and inhibitors towards combating leishmaniasis, *Acta Tropica*, 181, 95-104 DOI 10.1016/j.actatropica.2018.02.010.

(11) Khan, O. M. F. (2007) Trypanothione Reductase: A viable chemotherapeutic target for antitrypanosomal and antileishmanial drug design, *Drug Target Insights* 2, 129-146 DOI 10.1177/117739280700200007.

(12) Bernardes, L. S. C., Zani, C. L., Carvalho, I. (2013) Trypanosomatidae diseases: from the current therapy to the efficacious role of trypanothione reductase in drug discovery. *Curr. Med. Chem.* 20, 2673-2696 DOI 10.2174/0929867311320210005.

(13) Tiwari, N., Tanwar, N., Munde, M. (2018) Molecular insights into trypanothione reductase-inhibitor interaction: A structure-based review. *Arch. Pharm. Chem. Life Sci.* 351, 1-12 DOI 10.1002/ardp.201700373.

(14) Toro, M., Sánchez-Murcia, P. A., Moreno. D., Ruiz-Santaquiteria., M., Alzate, J. F., Negri, A., Camarasa, M. J., Gago, F., Velázquez, S., Jiménez-Ruiz, A. (2013) Probing the dimerization interface of *Leishmania infantum* trypanothione reductase with site-directed mutagenesis and short peptides, *ChemBioChem* 14, 1212-1217 DOI 10.1002/cbic.201200744.

(15) Sánchez-Murcia, P. A., Ruiz-Santaquiteria, M., Toro, M., de Lucio, H., Jiménez, M. A., Gago, F., Jiménez-Ruiz, A., Camarasa, M. J., Velázquez, S. (2015) Comparison of hydrocarbon- and lactam-bridged cyclic peptides as dimerization inhibitors of *Leishmania infantum* trypanothione reductase, *RSC Adv*. 5, 55784-55794 DOI 10.1039/C5RA06853C.

(16) Ruiz-Santaquiteria, M., Sanchez-Murcia, P. A., Toro, M., de Lucio, H., Gutierrez, K.J., de Castro, S., Carneiro, F. A. C., Gago, F., Jiménez-Ruiz, A., Camarasa, M. J., Velázquez, S. (2017) First examples of peptides targeting the dimer interface of *Leishmania infantum* trypanothione reductase with potent in vitro antileishmanial activity. *Eur. J. Med. Chem.* 135, 49-59 DOI 10.1016/*j*.ejmech.2017.04.020.

(17) Ruiz-Santaquiteria, M., De Castro, S., Camarasa, M. J., Toro, M., de Lucio, H., Gutiérrez, K. J., Jiménez-Ruiz, A., Sánchez-Murcia, P. A., Gago, F., Jiménez, M. A., Velázquez, S. (2018) Trypanothione reductase inhibition and anti-leishmanial activity of all-hydrocarbon stapled α-helical peptides with improved proteolytic stability, *Eur. J. Med. Chem.* 149, 238-247 DOI 10.1016/j.ejmech.2018.02.071.

(18) De Lucio, H., Gamo, A., Ruiz-Santaquiteria, M., de Castro, S., Sánchez-Murcia, P. A., Toro, M., Gutiérrez, K. J., Gago, F., Jiménez-Ruiz, A., Camarasa, M. J., Velázquez, S. (2017) Improved proteolytic stability and potent activity against *Leishmania infantum* trypanothione reductase of α/β^3-peptide foldamers conjugated to cell-penetrating peptides, *Eur. J. Med. Chem.* 140, 615-623 DOI 10.1016/*j*.ejmech.2017.09.032.

(19) Davis, J. M., Tsou, L. K., Hamilton, A. D. (2007) Synthetic non-peptide mimetics of α-helices, *Chem. Soc. Rev.* 36, 326-334 DOI 10.1039/B608043J.

(20) Azzarito, V., Long, K., Murphy, N. S., Wilson, A. J. (2013) Inhibition of α-helix-mediated protein-protein interactions using designed molecules. *Nat. Chem.* 5, 161-173 DOI 10.1038/nchem.1568.

(21) Milroy, L. G., Grossmann, T. N., Hennig, S., Brunsveld, L., Ottmann, C. (2014) Modulators of protein-protein interactions, *Chem. Rev.* 114, 4695-4748 DOI 10.1021/cr400698c.

(22) Sheng, C., Dong, G., Miao, Z., Zhang, W., Wang, W. (2015) State-of-the-art strategies for targeting protein-protein interactions by small-molecule inhibitors, *Chem. Soc. Rev.* 44, 8238-8259 DOI 10.1039/C5CS00252D.

(23) Orner, B. P., Ernst, J. T., Hamilton, A. D. (2001) Toward proteomimetics: Terphenyl derivatives as structural and functional mimics of extended regions of an α-helix. *J. Am. Chem. Soc.* 123, 5382-5383 DOI 10.1021/ja0025548.

(24) Jayatunga, M. K. P., Thompson, S., Hamilton, A. D. (2014) α-helix mimetics: outwards and upwards, *Bioorg. Med. Chem.* 24, 717-724 DOI 10.1016/j.bmcl.2013.12.003.

(25) Wilson, A. J. (2015) Helix mimetics: recent developments, *Progress Biophys. Mol. Biol.* 119, 33-40 DOI 10.1016/j.pbiomolbio.2015.05.001.

(26) Davis, J. M., Truong, A., Hamilton, A. D. (2005) Synthesis of 2,3'; 6',3"-Terpyridine scaffold as an α-helix mimetic, *Org. Lett.* 7, 5405-5408 DOI 10.1021/ol0521228.

(27) Yin, H., Lee, G. I., Sedey, K. A., Rodríguez, J. M., Wang, H. G., Sebti, S. M., Hamilton, A. D. (2005) Terephthalamide derivatives as mimetics of helical peptides: disruption of the Bcl-x(L)/Bak interaction. *J. Am. Chem. Soc.* 127, 5463-5468 DOI 10.1021/ja0446404.

(28) Cummings, C. G., Ross, N. T., Katt, W. P., Hamilton, A. D. (2009) Synthesis and biological evaluation of a 5-6-5 imidazole-phenyl-thiazole based α-helix mimetic, *Org. Lett.* 11, 25-28 DOI 10.1021/ol8022962.

(29) Cummings, C. G., Hamilton, A. D. (2013) Expedient route to functionalized and water soluble 5-6-5 imidazole-phenyl-thiazole based α-helix mimetics, *Tetrahedron* 69, 1663-1668 DOI 10.1016/j.tet.2012.11.070.

(30) Campbell, F., Plante, J. P., Edwards, T. A., Warriner, S. L., Wilson, A. J. (2010) *N*-alkylated oligoamide α-helical proteomimetics. *Org. Biomol. Chem.* 8, 2344-2351 DOI 10.1039/C001164A.

(31) Long, K., Edwards, T. A., Wilson, A. J. (2013) Microwave assisted solid phase synthesis of highly functionalized N-alkylated oligobenzamide α-helix mimetics. *Bioorg. Med. Chem.* 21, 4034-4040 DOI 10.1016/j.bmc.2012.09.053.

(32) Lee, J. H., Zhang, Q., Jo, S., CHai, S. C., Oh, M., Im, W., Lu, H., Lim, H-S. (2011) Novel pyrrolopyrimidine-based α-helix mimetics: cell-permeable inhibitors of protein-protein interactions. *J. Am. Chem. Soc.* 133, 676-679 DOI 10.1021/ja108230s.

(33) Lee, J. H., Lim, H-S. (2012) Solid-phase synthesis of tetrasubstituted pyrrolo[2,3-*d*]pyrimidines. *Org. Biomol. Chem.* 10, 4229-4235 DOI 10.1039/C2OB06899K.

(34) Antuch, W., Menon, S., Chen, Q-Z., Lu, Y., Sakamuri, S., Beck, B., Schauer-Vukasinovic, V., Agarwal, S., Hess, S., Dömling, A. (2006) Design and modular parallel synthesis of a MCR derived

α-helix mimetic protein-protein interaction inhibitor scaffold. *Bioorg. Med. Chem. Lett.* 16, 1740-1743 DOI 10.1016/j.bmcl.2005.11.102.

(35) Pelay-Gimeno, M., Glas, A., Koch, O., Grossmann, T. N. (2015) Structure-based design of inhibitors of protein-protein interactions: mimicking peptide binding epitopes, *Angew. Chem. Int. Ed.* 54, 8896-8927 DOI 10.1002/anie.201412070.

(36) For a representative example see: Lao, B. B., Grishagin, I., Mesallati, H., Brewer, T. F., Olenyuuk, B. Z., Arora, P. S. (2014) In vivo modulation of hypoxia-inducible signaling by topographical helix mimetics. *Proc. Natl. Acad. Sci USA* 111, 7531-7536 DOI 10.1073/pnas.1402393111.

(37) Rogers, J. F., Green, D. M. (2002) Mild conversion of electron deficient aryl fluorides to phenols using 2-(methylsulfonyl)ethanol. *Tetrahedron Lett.* 43, 3585-3587 DOI 10.1016/S0040-4039(02)00561-0.

(38) For reviews see for example: a) Das, P., Sharma, D., Kumar, M., Singh, B. (2010) Copper promoted C-N and C-O type cross-coupling reactions. *Curr. Org. Chem.* 14, 754-783 DOI 10.2174/138527210791111830; b) Bhunia, S., Pawar, G. G., Kumar, S. V., Jiang, Y. (2017) Selected copper-based reactions for C-N, C-O, C-S and C-C bond formation. *Angew. Chem. Int. Ed.* 56, 16136-16179 DOI 10.1002/anie.201701690.

(39) Zhang, H., Cai, Q., Ma, D. (2005) Amino acid promoted CuI-catalyzed C-N bond formation between aryl halides and amines or N-containing heterocycles. *J. Org. Chem.* 70, 5164-5173 DOI 10.1021/jo0504464.

(40) Ngo, Q. A., Nguyen, L. A., Vo, N. B., Nguyen, T. H., Rous, F., Nguyen, T. H., Nguyen, V. T. (2015) Synthesis and antiproliferative activity of new vinca alkaloids containing an α,β-unsaturated aromatic side chain. *Bioorg. Med. Chem. Lett.* 25, 5597-5600 DOI 10.1016/j.bmcl.2015.10.040.

(41) Hamilton, C. J., Saravanamuthu, A., Eggleston, I. M., Fairlamb, A. H. (2003) Ellman's-reagent-mediated regeneration of trypanothione in situ: substrate-economical microplate and time-

dependent inhibition assays for trypanothione reductase. *Biochem. J.*, 369, 529-537 DOI 10.1042/BJ20021298.

(42) Saravanamuthu, A., Vickers, T. J., Bond, C. S., Peterson, M. R., Hunter, M. N., Fairlamb, A. H. (2004). Two Interacting Binding Sites for Quinacrine Derivatives in the Active Site of Trypanothione Reductase. *J. Biol. Chem.* 28, 29493-29500 DOI 10.1074/jbc.M403187200.

(43) De Gasparo, R., Brodbeck-Persch, E., Bryson, S., Hentzen, N. B., Kaiser, M., Pai, E. F., Krauth-Siegel, R. L., Diederich, F. (2018) Biological evaluation and X-ray Co-crystal structures of cyclohexylpyrrolidine ligands for trypanothione reductase, an enzyme from the redox metabolism of Trypanosoma. *ChemMedChem* 13, 957-967 DOI: 10.1002/cmdc.201800067.

(44) Persch, E., Bryson, S., Todoroff, N. K., Eberle, C., Thelemann, J., Dirdjaja, N., Kaiser, M., Weber, M., Derbani, H., Brun, R., Schneider, G., Pai, E. F., Krauth-Siegel, R. L., Diederich, F. (2014) Binding to large enzyme pockets: Small-molecule inhibitors of trypanothione reductase. *ChemMedChem* 9, 1880-1891 DOI: 10.1002/cmdc.201402032

(45) Hurevich, M., Tal-Gan, Y., Klein, S., Barda, Y., Levitzki, A., Gilon, C. (2010) Novel method for the synthesis of urea backbone cyclic peptides using new Alloc-protected glycine building units. *J. Pept. Sci.* 16, 178-185 DOI 10.1002/psc.1218.

(46) Bionda, N., Pitteloud, J-P., Cudic, P. (2013) Solid-phase synthesis of fusaricidin/LI-F class of cyclic lipopeptides: guanidinylation of resin-bound peptidyl amines. *Biopolymers*. 100 (2), 160-166 DOI 10.1002/bip.22186.

(47) Alzate, J. F., Arias, A., Mollinedo, F., Rico, E., de la Iglesia-Vicente, J., Jimenez-Ruiz, A. (2008) Edelfosine induces an apoptotic process in *Leishmania infantum* that is regulated by the ectopic expression of Bcl-XL and Hrk. *Antimicrob. Agents Chemother.* 52(10), 3779-3792 DOI 10.1128/AAC.01665-07.

(48) Kabsch, W. (2010) *XDS. Acta Cryst.* D66, 125-132 DOI 10.1107/S0907444909047337.

(49) Winn, M. D., Ballard, C. C., Cowtan, K. D., Dodson, E. J., Emsley, P., Evans, P. R., Keegan, R.M., Krissinel, E. B., Leslie, A. G. W., McCoy, A., McNicholas, S. J., Murshudov, G. N., Pannu, N. S., Potterton, E. A., Powell, H. R., Read, R. J., Vagin, A., Wilsonc, K. S. (2011) Overview of the CCP4 suite and current developments. *Acta. Cryst.* D67, 235-242 DOI 10.1107/S0907444910045749.

(50) Vagin, A. A., Teplyakov, A. (1997) MOLREP: an automated program for Molecular Replacement. *J. Appl. Cryst.* 30, 1022 – 1025 DOI 10.1107/S0021889897006766.

(51) Murshudov, G. N., Skubak, P., Lebedev, A. A., Pannu, N. S., Steiner, R. A., Nicholls, R. A., Winn, M. D., Long, F., Vagin, A. A. (2011) REFMAC5 for the refinement of macromolecular crystal structures. *Acta Cryst.* D67, 355-367 DOI 10.1107/S0907444911001314.

(52) Emsley P., Cowtan K. (2004) Coot: model-building tools for molecular graphics. *Acta Crystallogr D Biol Crystallogr.* 60, 2126–32 DOI 10.1107/S0907444904019158.

(53) Baiocco, P., Colotti, G., Franceschini, S., Ilari, A., (2009) Molecular basis of antimony treatment in leishmaniasis. *J. Med. Chem.* 52 (8), 2603-2612 DOI 10.1021/jm900185q

(54) Klett, J., Núñez-Salgado, A., Dos Santos, H. G., Cortés-Cabrera, A., Perona, A., Gil-Redondo, R., Abia, D., Gago, F., Morreale, A. (2012) MM-ISMSA: an ultrafast and accurate scoring function for protein-protein docking. *J. Chem. Theory Comput.* 8 (9), 3395-3408 DOI 10.1021/ct300497z.

(55) Wolber, G., Langer, T. (2005) LigandScout: 3-D pharmacophores derived from protein-bound ligands and their use as virtual screening filters. *J. Chem. Inf. Model.* 45 (1), 160-169 DOI 10.1021/ci049885e.

Table of contents (TOC)